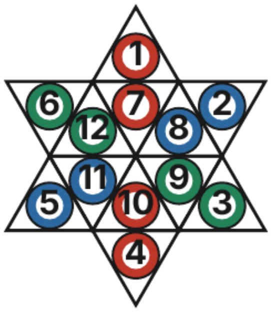

STAR FACE

Polyhedral Sieve Model for Medical Diagnostics

Catalogue of 2D star faces (hexagrams) on a 3D polyhedron (Escher’s solid)

Families, groupings, masked rare diseases and the three-stage sieve

---

Equilibrium · Unambiguity · Reliability

Introducing

summetry

(n., coined from “sum+symmetry”)

Grego

Földvári Gergely · grego.hu ·

grego.hu/star

"When you hear hoofbeats, think of horses, not zebras!"

— a medical-school diagnostic principle (T. E. Woodward)

The Little Prince on Asteroid B-612 — surveying his whole small world from one spot

Antoine de Saint-Exupéry · The Morgan Library & Museum, New York (MA 2592.34)

Dedicated to my father and mother, Péter and Vera,
and to my children, Fanni and Sámuel.

Contents

Ars longa, vita brevis — Hippocrates (c. 400 BC)

INTRODUCTION

On the other half of our planet, Bolt, Eggleton and Gilks had defined what a magic hexagram was (B. Bolt, R. Eggleton and J. Gilks, "The Magic Hexagram," Mathematical Gazette 75, 141–142, 1991).

Here and now, I take up that definition more broadly, and mount the hexagram on a concave polyhedron that tiles space: Escher's solid, the stellated rhombic dodecahedron, seen also as the invaginated cuboctahedron and as the compound of three flattened octahedra. Its forty-eight faces, read through the star, are the subject of this book.

My aim, however, is beyond recreational mathematics: an intuition induced by personal experience tells me that this extraordinary solid has properties that can help symbolically model a system of sieves on solid logical grounds, which can open the way to a more efficient way of thinking about modern-day medical diagnostics, potentially helping achieve higher success with the diagnoses of rare diseases, so often in disguise.

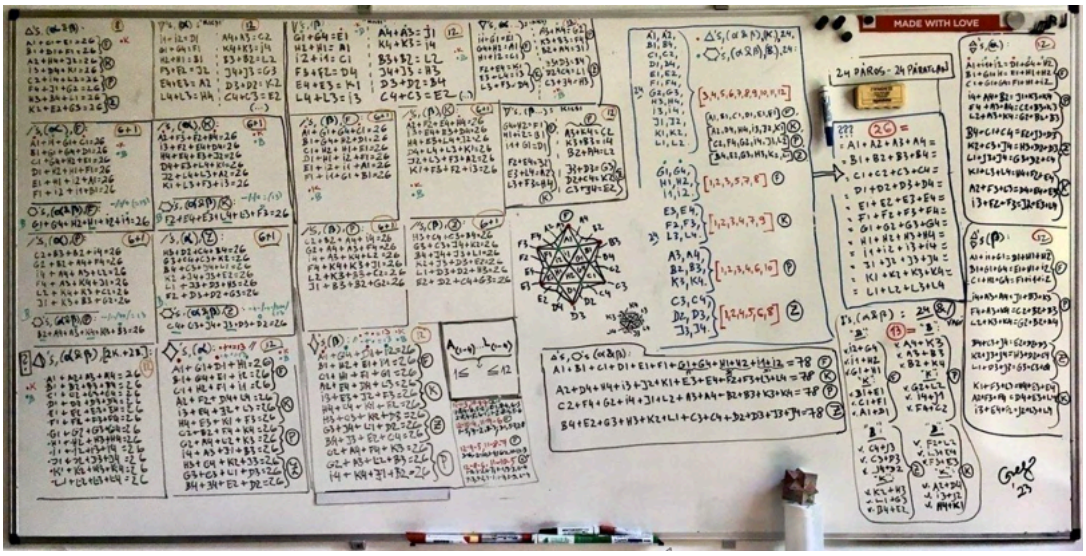

Early research on whiteboard: Diophantine equations and the solid (Grego, 2023)

HOW TO READ THIS BOOK

(Fast lane: skip to "Zeroth Sieve", page 26, for quick answers)

The hexagram star has twelve faces. The six outer tips are numbered 1 to 6 and the six inner faces 7 to 12, clockwise from the top. A face keeps its number throughout the book. Colour marks the group a face belongs to. Where a face belongs to two groups at once its disc is split between the two colours.

While the new English mosaic word ***summetry*** (perhaps coined here for the first time) may present far-reaching uses in various scientific, artistic and other contexts, the reader deserves to know that the paper's central concept of a *sieve* means heart (*szív*) when pronounced in the author's native Hungarian language.

Two levels are catalogued. First, the individual tuples of faces, gathered into symmetry families, i.e. sets of tuples that are images of one another under a mirror or a turn. Second, the groupings: complete covers and partitions of all twelve faces by a single symmetry family.

Stage one presents these groupings, stage two applies the zeroth, the equilibrium, the unambiguity and the reliability sieves by the numbering of faces with values and their magic sums. Stage three presents the author's related works and spin-offs that were and are researched along the way.

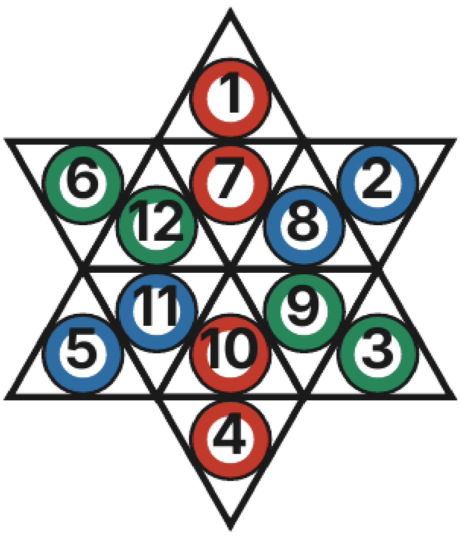

The Diaquad Star Face

In this example, the *diaquad* (diametric quadruple) star's twelve congruent, regular triangle (appearing) faces are numbered from one to twelve, going clockwise. This core numbering is used for identifying the twelve faces, so (1,4,7,10), (2,5,8,11), (3,6,9,12) indicate the three diaquads.

Disregarding colors, e.g. (1,7) is a pair, (1,3,8) a triple, (1,3,7,9) a quadruple, (3,5,9,10,11) a quintuple and (2,4,6,8,10,12) a sextuple. Escher's solid, the polyhedron sieved for the diagnosis model shows such hexagrams orthographically (on a vertical projection plane in front of a viewer).

The shapes at a glance

one dot marks each group a face belongs to; two marks an overlap

Partitions — every face once

two by six

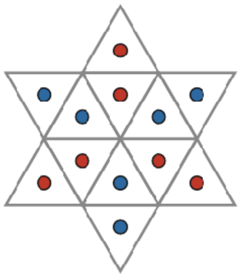

39

three by four

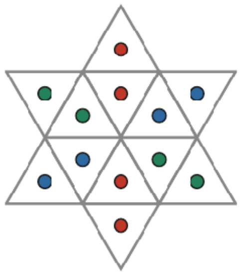

26

six by two

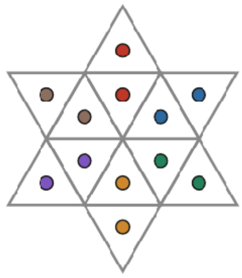

13

Covers — faces shared between groups

six by three

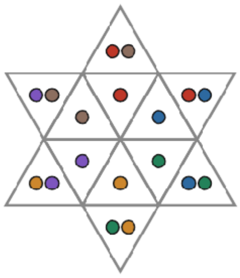

17–22

six by four

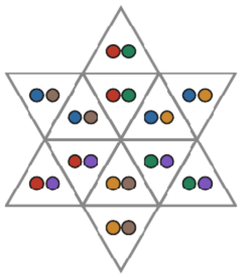

26

six by five

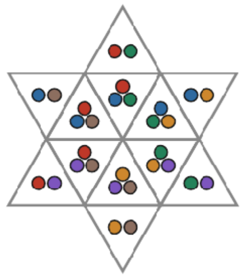

32/33

The constants shown are the equilibrial sums reached in Stage Two (see pages 28–34). One shape, four groups of three, is absent: it can never balance, and is set aside by the sieve.

THE COUNTS

how many of each, on the fixed star and up to symmetry

Families of tuples, by size

size	1	2	3	4	5	6
tuples	12	66	220	495	792	924
families	2	10	24	54	76	96

Groupings of all twelve faces

shape	kind	distinct	up to symmetry
two by six	partition	104	22
three by four	partition	27	10
six by two	partition	10	6
four by three	partition	0	0
six by three	cover	54	30
six by four	cover	145	81
six by five	cover	294	156

‘Distinct’ counts each placement on the fixed star; ‘up to symmetry’ collapses rotations and mirrors to one. Four groups of three yields nothing: no four triples are ever a single symmetry family. Four alone does not divide the star’s six-fold turn (60°, 120°, 180°, 240°, 300°). There is no quarter-turn (90°, 180°, 270°) to carry four groups one onto the next, so four threes can never be symmetric. My sieve logic later bars this same shape by arithmetic, too; symmetry and balance (equilibrium) fail together, *summetry* is missing.

By 2D and 3D *summetry*, respectively, the 7–11 families complement the sums of 5–1, with 6–6 in the middle, producing no new counts or magic-sum values, while the 13 rotational symmetry axes each have a perpendicular plane — 9 mirror, 4 roto-reflective — cutting the solid into two congruent halves.

Single faces

Two families: the six outer tips, and the six inner faces.

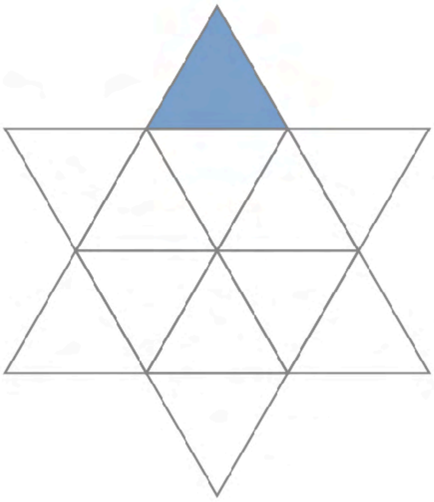

{1} · ×6

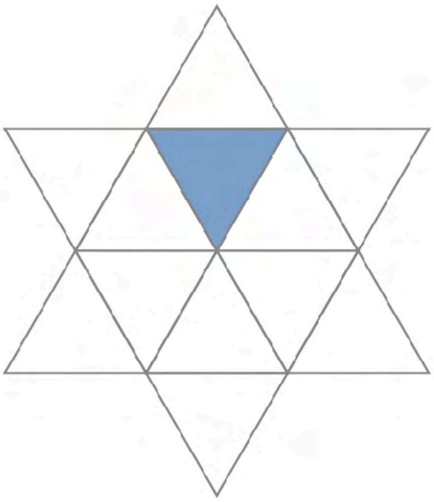

{7} · ×6

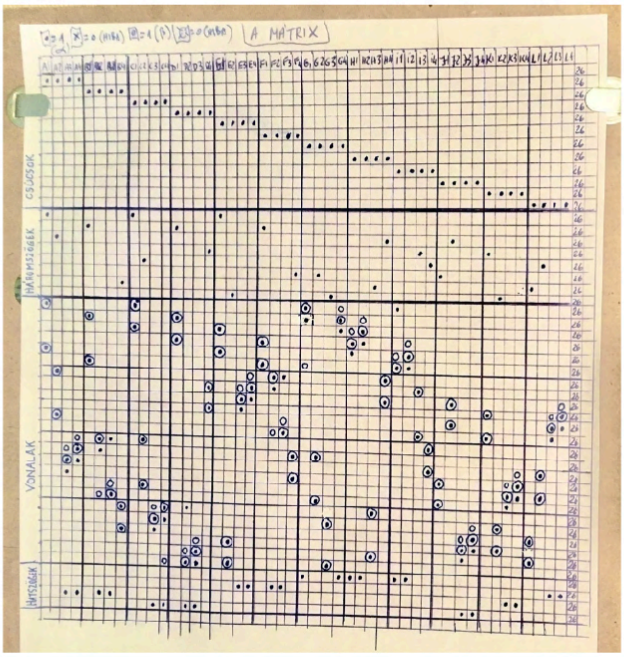

Early research: an attempted Gauss-elimination solution for the Diophantine equation system on paper

— Grego

Pairs

Ten families of paired faces — radial, antipodal, adjacent, and the rest.

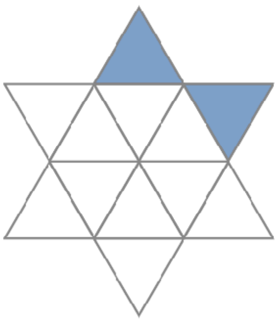

{1,2} · ×6

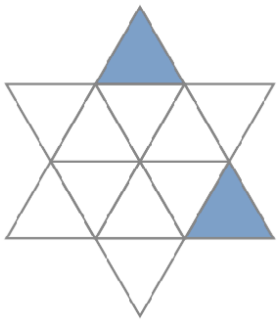

{1,3} · ×6

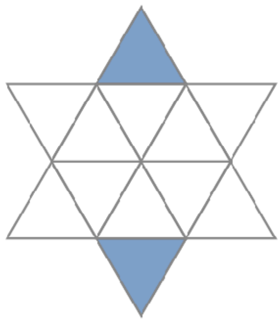

{1,4} · ×3

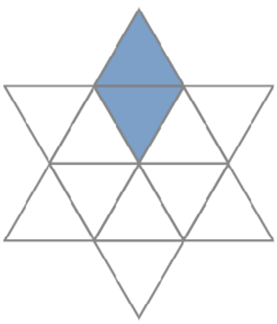

{1,7} · ×6

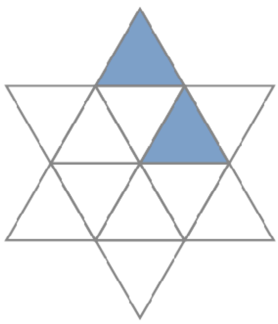

{1,8} · ×12

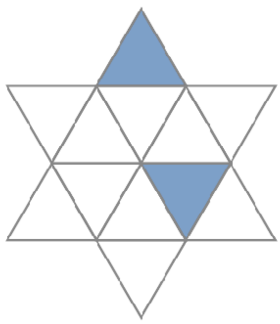

{1,9} · ×12

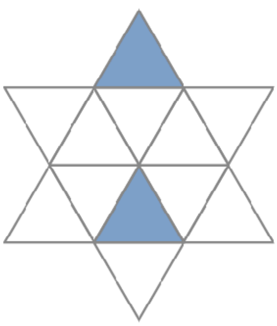

{1,10} · ×6

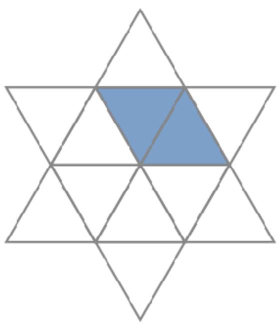

{7,8} · ×6

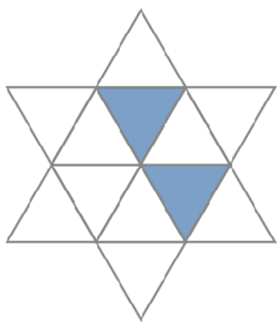

{7,9} · ×6

Pairs (continued)

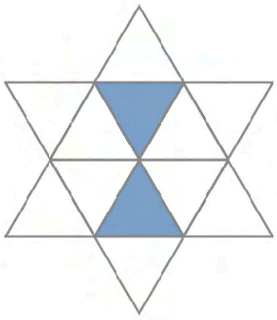

{7,10} · ×3

Sometimes it really is a zebra.

— Grego

Triples

Twenty-four families of triples.


{1,2,3} · ×6


{1,2,4} · ×12


{1,2,7} · ×12


{1,2,9} · ×12


{1,2,10} · ×12


{1,3,5} · ×2


{1,3,7} · ×12


{1,3,8} · ×6


{1,3,10} · ×12


{1,3,11} · ×6


{1,4,7} · ×6


{1,4,8} · ×12


{1,7,8} · ×12


{1,7,9} · ×12


{1,7,10} · ×6


{1,8,9} · ×12

Triples (continued)

{1,8,10} · ×12

{1,8,11} · ×12

{1,8,12} · ×6

{1,9,10} · ×12

{1,9,11} · ×6

{7,8,9} · ×6

{7,8,10} · ×12

{7,9,11} · ×2

A small world, surveyed from a single point.

Antoine de Saint-Exupéry · The Morgan Library & Museum

Quadruples

Fifty-four families of four.

{1,2,3,4} · ×6

{1,2,3,5} · ×6

{1,2,3,7} · ×12

{1,2,3,8} · ×6

{1,2,3,10} · ×12

{1,2,3,11} · ×6

{1,2,4,5} · ×3

{1,2,4,7} · ×12

{1,2,4,8} · ×12

{1,2,4,9} · ×12

{1,2,4,10} · ×12

{1,2,4,11} · ×12

{1,2,4,12} · ×12

{1,2,7,8} · ×6

{1,2,7,9} · ×12

{1,2,7,10} · ×12

{1,2,7,11} · ×12

{1,2,7,12} · ×12

{1,2,9,10} · ×12

{1,2,9,11} · ×12

Quadruples (continued)


{1,2,9,12} · ×6


{1,2,10,11} · ×6


{1,3,5,7} · ×6


{1,3,5,8} · ×6


{1,3,7,8} · ×12


{1,3,7,9} · ×6


{1,3,7,10} · ×12


{1,3,7,11} · ×12


{1,3,7,12} · ×12


{1,3,8,10} · ×12


{1,3,8,11} · ×6


{1,3,10,11} · ×12


{1,3,10,12} · ×6


{1,4,7,8} · ×12


{1,4,7,9} · ×12


{1,4,7,10} · ×3


{1,4,8,9} · ×6


{1,4,8,11} · ×6


{1,4,8,12} · ×6


{1,7,8,9} · ×12

Quadruples (continued)

{1,7,8,10} · ×12

{1,7,8,11} · ×12

{1,7,8,12} · ×6

{1,7,9,10} · ×12

{1,7,9,11} · ×6

{1,8,9,10} · ×12

{1,8,9,11} · ×12

{1,8,9,12} · ×12

{1,8,10,11} · ×12

{1,8,10,12} · ×6

{1,9,10,11} · ×6

{7,8,9,10} · ×6

{7,8,9,11} · ×6

{7,8,10,11} · ×3

Quintuples

Seventy-six families of five.

{1,2,3,4,5} · ×6

{1,2,3,4,7} · ×12

{1,2,3,4,8} · ×12

{1,2,3,4,11} · ×12

{1,2,3,5,7} · ×12

{1,2,3,5,8} · ×6

{1,2,3,5,10} · ×12

{1,2,3,5,11} · ×6

{1,2,3,7,8} · ×12

{1,2,3,7,9} · ×6

{1,2,3,7,10} · ×12

{1,2,3,7,11} · ×12

{1,2,3,7,12} · ×12

{1,2,3,8,10} · ×12

{1,2,3,8,11} · ×6

{1,2,3,10,11} · ×12

{1,2,3,10,12} · ×6

{1,2,4,5,7} · ×12

{1,2,4,5,9} · ×6

{1,2,4,7,8} · ×12

Quintuples (continued)


{1,2,4,7,9} · ×12


{1,2,4,7,10} · ×12


{1,2,4,7,11} · ×12


{1,2,4,7,12} · ×12


{1,2,4,8,9} · ×12


{1,2,4,8,10} · ×12


{1,2,4,8,11} · ×12


{1,2,4,8,12} · ×12


{1,2,4,9,10} · ×12


{1,2,4,9,11} · ×12


{1,2,4,9,12} · ×12


{1,2,4,10,11} · ×12


{1,2,4,10,12} · ×12


{1,2,4,11,12} · ×12


{1,2,7,8,9} · ×12


{1,2,7,8,10} · ×12


{1,2,7,9,10} · ×12


{1,2,7,9,11} · ×12


{1,2,7,9,12} · ×12


{1,2,7,10,11} · ×12

Quintuples (continued)

{1,2,7,10,12} · ×12

{1,2,7,11,12} · ×12

{1,2,9,10,11} · ×12

{1,2,9,10,12} · ×12

{1,3,5,7,8} · ×12

{1,3,5,7,9} · ×6

{1,3,5,7,10} · ×6

{1,3,5,8,10} · ×6

{1,3,7,8,9} · ×6

{1,3,7,8,10} · ×12

{1,3,7,8,11} · ×12

{1,3,7,8,12} · ×12

{1,3,7,9,10} · ×12

{1,3,7,9,11} · ×6

{1,3,7,10,11} · ×12

{1,3,7,10,12} · ×12

{1,3,7,11,12} · ×12

{1,3,8,10,11} · ×12

{1,3,8,10,12} · ×6

{1,3,10,11,12} · ×6

Quintuples (continued)


{1,4,7,8,9} · ×12


{1,4,7,8,10} · ×12


{1,4,7,8,11} · ×12


{1,4,7,8,12} · ×6


{1,4,7,9,11} · ×6


{1,4,8,9,11} · ×12


{1,7,8,9,10} · ×12


{1,7,8,9,11} · ×12


{1,7,8,9,12} · ×12


{1,7,8,10,11} · ×12


{1,7,8,10,12} · ×6


{1,7,9,10,11} · ×6


{1,8,9,10,11} · ×12


{1,8,9,10,12} · ×12


{1,8,9,11,12} · ×6


{7,8,9,10,11} · ×6

Sixes

Ninety-six families of six, including the two whole rings, kept here and marked invariant.


{1,2,3,4,5,6} · ×1 inv


{1,2,3,4,5,7} · ×12


{1,2,3,4,5,8} · ×12


{1,2,3,4,5,9} · ×6


{1,2,3,4,5,12} · ×6


{1,2,3,4,7,8} · ×12


{1,2,3,4,7,9} · ×12


{1,2,3,4,7,10} · ×6


{1,2,3,4,7,11} · ×12


{1,2,3,4,7,12} · ×12


{1,2,3,4,8,9} · ×6


{1,2,3,4,8,11} · ×12


{1,2,3,4,8,12} · ×12


{1,2,3,4,11,12} · ×6


{1,2,3,5,7,8} · ×12


{1,2,3,5,7,9} · ×6


{1,2,3,5,7,10} · ×12


{1,2,3,5,7,11} · ×12


{1,2,3,5,7,12} · ×12


{1,2,3,5,8,10} · ×12

Sixes (continued)


{1,2,3,5,8,11} · ×6


{1,2,3,5,10,11} · ×12


{1,2,3,5,10,12} · ×6


{1,2,3,7,8,9} · ×6


{1,2,3,7,8,10} · ×12


{1,2,3,7,8,11} · ×12


{1,2,3,7,8,12} · ×12


{1,2,3,7,9,10} · ×12


{1,2,3,7,9,11} · ×6


{1,2,3,7,10,11} · ×12


{1,2,3,7,10,12} · ×12


{1,2,3,7,11,12} · ×12


{1,2,3,8,10,11} · ×12


{1,2,3,8,10,12} · ×6


{1,2,3,10,11,12} · ×6


{1,2,4,5,7,8} · ×6


{1,2,4,5,7,9} · ×12


{1,2,4,5,7,10} · ×6


{1,2,4,5,7,11} · ×6


{1,2,4,5,7,12} · ×12

Sixes (continued)


{1,2,4,5,9,12} · ×3


{1,2,4,7,8,9} · ×12


{1,2,4,7,8,10} · ×12


{1,2,4,7,8,11} · ×12


{1,2,4,7,8,12} · ×12


{1,2,4,7,9,10} · ×12


{1,2,4,7,9,11} · ×12


{1,2,4,7,9,12} · ×12


{1,2,4,7,10,11} · ×12


{1,2,4,7,10,12} · ×12


{1,2,4,7,11,12} · ×12


{1,2,4,8,9,10} · ×12


{1,2,4,8,9,11} · ×12


{1,2,4,8,9,12} · ×12


{1,2,4,8,10,11} · ×12


{1,2,4,8,10,12} · ×12


{1,2,4,8,11,12} · ×12


{1,2,4,9,10,11} · ×12


{1,2,4,9,10,12} · ×12


{1,2,4,9,11,12} · ×12

Sixes (continued)

{1,2,4,10,11,12} · ×12

{1,2,7,8,9,10} · ×12

{1,2,7,8,9,11} · ×12

{1,2,7,8,9,12} · ×6

{1,2,7,8,10,11} · ×6

{1,2,7,9,10,11} · ×12

{1,2,7,9,10,12} · ×12

{1,2,7,9,11,12} · ×12

{1,2,7,10,11,12} · ×12

{1,2,9,10,11,12} · ×6

{1,3,5,7,8,9} · ×6

{1,3,5,7,8,10} · ×12

{1,3,5,7,8,11} · ×12

{1,3,5,7,8,12} · ×6

{1,3,5,7,9,11} · ×2

{1,3,5,8,10,12} · ×2

{1,3,7,8,9,10} · ×12

{1,3,7,8,9,11} · ×6

{1,3,7,8,10,11} · ×12

{1,3,7,8,10,12} · ×12

Sixes (continued)


{1,3,7,8,11,12} · ×12


{1,3,7,9,10,11} · ×12


{1,3,7,9,10,12} · ×6


{1,3,7,10,11,12} · ×12


{1,3,8,10,11,12} · ×6


{1,4,7,8,9,10} · ×6


{1,4,7,8,9,11} · ×12


{1,4,7,8,9,12} · ×12


{1,4,7,8,10,11} · ×6


{1,4,7,8,10,12} · ×6


{1,4,8,9,11,12} · ×3


{1,7,8,9,10,11} · ×12


{1,7,8,9,10,12} · ×12


{1,7,8,9,11,12} · ×6


{1,8,9,10,11,12} · ×6


{7,8,9,10,11,12} · ×1 inv

THE GROUPINGS

The Diaquads

three groups of four, one along each diameter ({3×4})

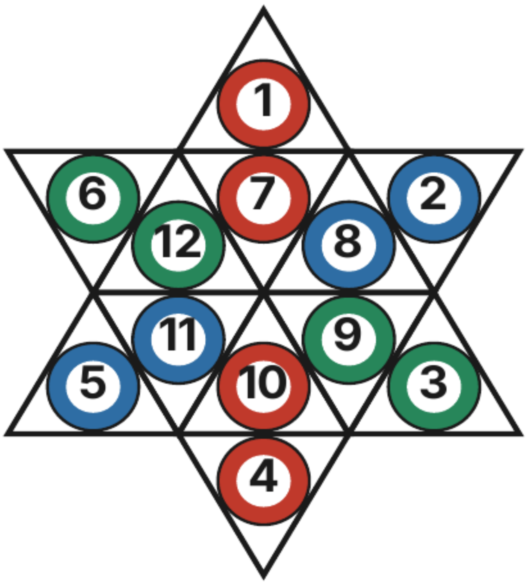

Each of the three diameters carries four faces. A 60° turn maps one diameter onto the next, so the three groups are images of one another. They form a single symmetry family, not an arbitrary division. The diaquads are one instance of SUMMETRY (defined at the equilibrial sieve), not the whole of it. Twenty-seven such partitions stand on the fixed star; ten distinct up to symmetry.

THE GROUPINGS (continued)

The David partition

two interlocking sixes ({2×6})

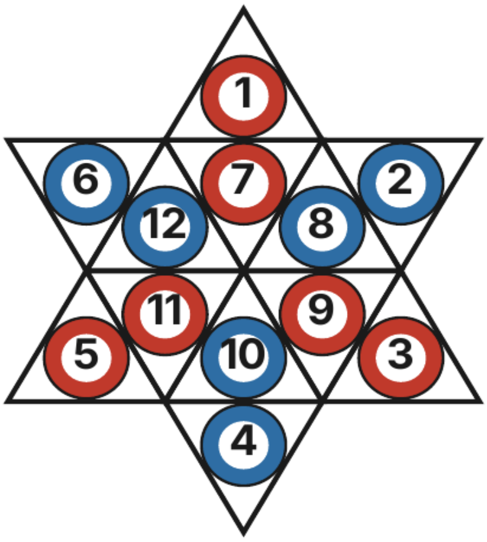

The twelve faces split into two sets of six that interlock as the two triangles of the star. A turn of 60° carries one set onto the other, so the pair forms one symmetry family. The inside–outside split, by contrast, is not a family: nothing carries the outer ring onto the inner. One hundred and four such partitions on the fixed star; twenty-two distinct up to symmetry.

THE GROUPINGS (continued)

The Star Lines

six groups of three along the edges ({6×3})

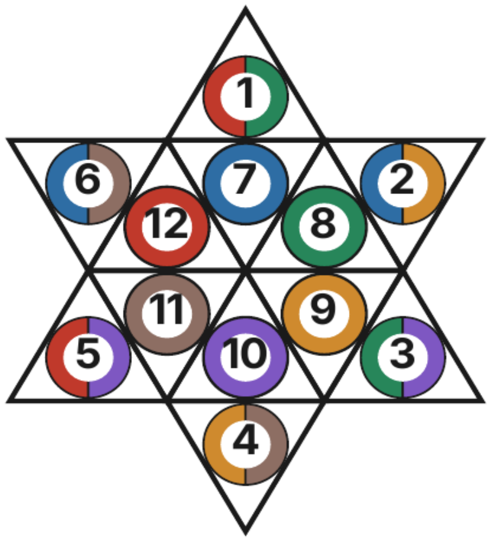

The six edges of the two triangles each gather three faces. Turning one edge by 60° gives the next, so the six form a family; the tips, lying on two edges apiece, carry two colours. Fifty-four such covers on the fixed star; thirty distinct up to symmetry.

THE GROUPINGS (continued)

The Dudeney hexagram

six lines of four, every face twice ({6×4})

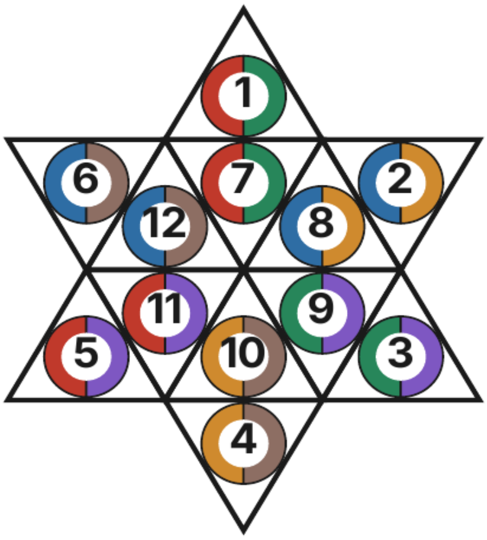

Six lines of four faces cover the star so that every face lies on exactly two lines. This is the classical magic-hexagram skeleton; in Stage Two it is the cover that balances at twenty-six. One hundred and forty-five such covers sit on the fixed star, of which eightyone are essentially different. (These count the patterns themselves, not their numberings.)

Henry Ernest Dudeney (1857–1930) was an English author and mathematician known as one of the foremost creators of mathematical puzzles in history.

→ THE ZEROTH SIEVE (Fast Lane Readers start here)

Why Escher's Solid

The three dimensions are treated here as the Universe, the all-encompassing space, with a single human observing it from a fixed point. The orthographic projection into two dimensions represents, in this model, the human cognitive-development process: the slow flattening of a vast world into something a mind can hold. The vector equilibrium is a cuboctahedron with all 12 of its identical vertices connected to the centre, being the only polyhedron with all edges and vectors equal in length, and it is the convex hull of Escher's Solid, an absolute omnidirectional balance.

I chose Escher's Solid because it originates closely in the cube; because it is a space-filling polyhedron, and an extreme one; and because it casts orthographic projections that are achiral polygons carrying a variety of rotational symmetries:

Projected polygon	Triangular faces	Projections	Rot. symmetry
square	16	6	90°
hexagram	12	8	60°
decagon	16	12	180°

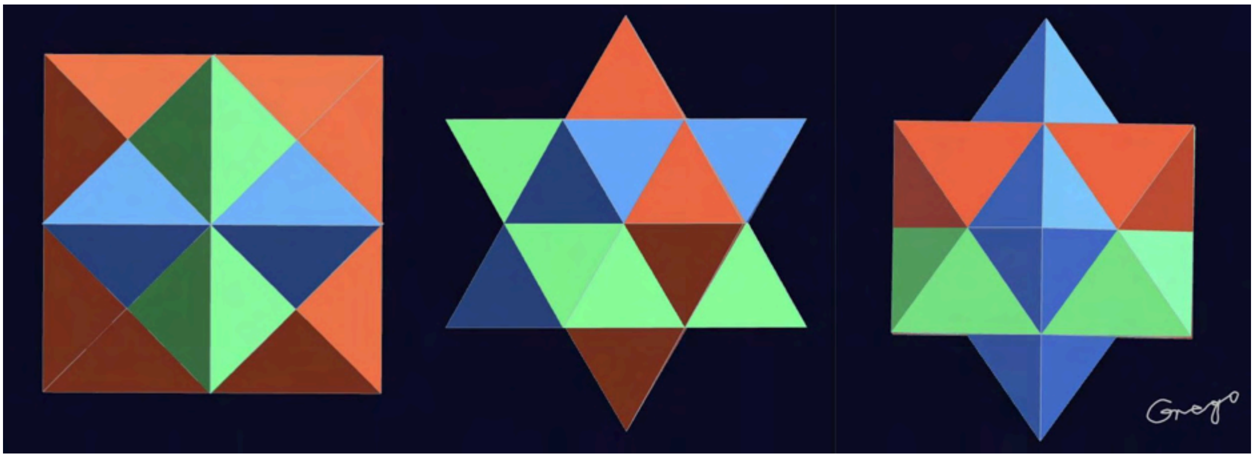

Screenshots of the solid's three orthographic projections from the
CUBE 2 ESCHER interactive 3D animation series by the author at
https://www.grego.hu/star

Why the hexagram

Of the three projected polygons, only the hexagram can cover the entire realm (all forty-eight faces) by disjoint projections: four disjoint hexagrams, at the least.

The squares and the decagons always hide some of the solid's faces; no set of them, however chosen, shows every face exactly once. This is confirmed by direct visibility computation on the solid. A square projection (a four-fold axis) shows sixteen faces, and there are six such views; no three disjoint squares reach forty-eight. A decagon projection (a two-fold axis) likewise shows sixteen faces across twelve views, and again no three disjoint decagons reach forty-eight.

A hexagram projection (a three-fold axis) shows twelve faces across eight views, and four of them, the eight viewing axes restricted to one inscribed tetrahedron, are mutually disjoint and together show all forty-eight. The hexagram alone tiles the whole realm.

The magic sum

Any magic sum feasible on the solid's twelve pyramids (its stellations) is the model's symbolic representation for the tested reliability of a diagnostic tool: one with an established full or partial correlation-system tied to known medical conditions.

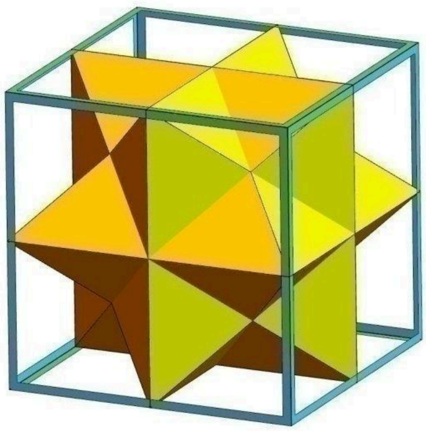

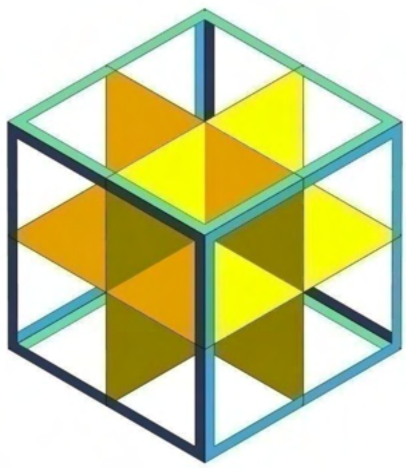

Escher's Solid within its cube (left); the hexagram projection along a three-fold axis (right).

by Sándor Kabai (1946-2024)

THE EQUILIBRIAL SIEVE

A grouping survives this first sieve if some numbering of the faces by the values one to twelve makes all of its groups share a single 'magic' sum, an equilibrium. It is set aside only when no numbering can ever do so.

I call this the SUMMETRY: a grouping that balances because it is symmetric and, as we'll see, is achiral. The sum arises from the symmetry itself. Every survivor of this sieve is an instance of it, the diaquads among them, not it alone.

The test is plain arithmetic

The values one to twelve total seventy-eight. A partition into n groups can balance only when seventy-eight divides evenly by n; so four groups of three (which would need 19.5) and twelve single faces (6.5) are impossible, and are sieved out. Every other shape can balance, each at its own constant.

The survivors balance at thirteen, seventeen to twenty-two*, twenty-six, thirtytwo or thirty-three* and thirty-nine. No constant is favoured; twenty-six is simply where two of the shapes happen to land. Should a later, independent condition single it out, that will be earned, not assumed.

In the language of the model: the sieve discards only the structurally impossible (the weight taken with bricks in the pocket, the body height measured together with that of shoe heels, the blood sample mixed with wine) and plays no favourites among results that are internally consistent.

On the sieves themselves: they are in a logic based chain and embed the constrained threshold set by the present state of canonized science, superimposed on the solid's geometry, within the symbolic model.

The evenhandedness above holds only among the results which that threshold already admits; the threshold itself may not be neutral, per se, and is not claimed to be, it is the vision itself, the intuitive expression behind the model, but a dynamic one.

The model's dynamism will be illustrated by a brief account of frontline examples of medical diagnostic research and development, with some of the promising mavericks figuratively mounted on the stellations, the four-faced pyramids under the twelve outer apexes of Escher's solid.

* BPS and VC calculations used to solve linear equal-sum constraints over a permutation of 1–12, with a Diophantine divisibility core (see page 38).

Six pairs

six pairs, each summing to thirteen ({6×2})

every group sums to 13

The groups

{1, 7} = 1 + 12 = 13

{2, 8} = 2 + 11 = 13

{3, 9} = 3 + 10 = 13

{4, 10} = 4 + 9 = 13

{5, 11} = 5 + 8 = 13

{6, 12} = 6 + 7 = 13

Each radial pair sums to thirteen.

Three diameters

three groups of four, each summing to twenty-six ({3×4})

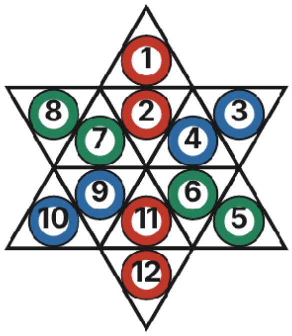

every group sums to 26

The groups

{1, 7, 10, 4} = 1 + 2 + 11 + 12 = 26

{2, 8, 11, 5} = 3 + 4 + 9 + 10 = 26

{3, 9, 12, 6} = 5 + 6 + 7 + 8 = 26

One of thirty-two value-partitions of the diaquads that balance at twenty-six.

Two halves

two interlocking sixes, each summing to thirty-nine ({2×6})

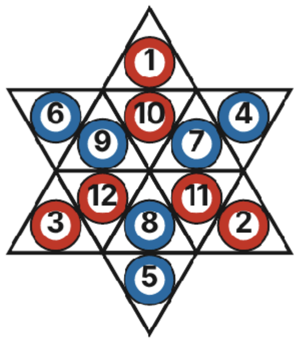

every group sums to 39

The groups

{1, 3, 5, 7, 9, 11} = 1 + 2 + 3 + 10 + 11 + 12 = 39

{2, 4, 6, 8, 10, 12} = 4 + 5 + 6 + 7 + 8 + 9 = 39

Each half of the David partition sums to thirty-nine.

Six triples

six groups of three, each summing to seventeen ({6×3})

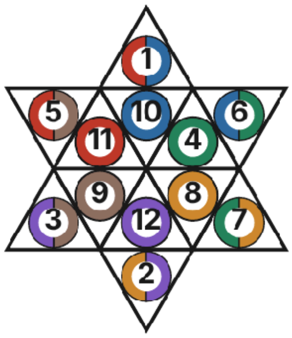

every group sums to 17

The groups

{1, 6, 12} = 1 + 5 + 11 = 17

{1, 2, 7} = 1 + 6 + 10 = 17

{2, 3, 8} = 6 + 7 + 4 = 17

{3, 4, 9} = 7 + 2 + 8 = 17

{4, 5, 10} = 2 + 3 + 12 = 17

{5, 6, 11} = 3 + 5 + 9 = 17

Twelve of the fifty-four covers of this shape admit a balanced numbering.

Footnote: the six triples are the loosest cover — they balance across the whole band 17–22 ($S = 13 + A/6$, as the outer ring's sum A runs 24, 30, …, 54). The six constants pair by complementation ($v \to 13-v$): 17→22, 18→21, 19→20. Seventeen, shown above, is the minimum.

Six lines

the Dudeney hexagram, every line summing to twenty-six ({6×4})

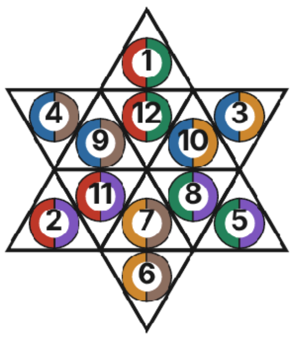

every group sums to 26

The groups

{1, 5, 7, 11} = 1 + 2 + 12 + 11 = 26

{2, 6, 8, 12} = 3 + 4 + 10 + 9 = 26

{1, 3, 7, 9} = 1 + 5 + 12 + 8 = 26

{2, 4, 8, 10} = 3 + 6 + 10 + 7 = 26

{3, 5, 9, 11} = 5 + 2 + 8 + 11 = 26

{4, 6, 10, 12} = 6 + 4 + 7 + 9 = 26

Every one of the six lines sums to twenty-six.

Six fives

six groups of five, balancing at thirty-two and thirty-three ({6×5})

every group sums to 33

every group sums to 32

The groups

- {1,5,7,11,12} = 1+8+9+3+12 = 33
- {2,6,7,8,12} = 4+2+9+6+12 = 33
- {1,3,7,8,9} = 1+10+9+6+7 = 33
- {2,4,8,9,10} = 4+11+6+7+5 = 33
- {3,5,9,10,11} = 10+8+7+5+3 = 33
- {4,6,10,11,12} = 11+2+5+3+12 = 33

The groups

- {1,5,7,11,12} = 12+5+4+10+1 = 32
- {2,6,7,8,12} = 9+11+4+7+1 = 32
- {1,3,7,8,9} = 12+3+4+7+6 = 32
- {2,4,8,9,10} = 9+2+7+6+8 = 32
- {3,5,9,10,11} = 3+5+6+8+10 = 32
- {4,6,10,11,12} = 2+11+8+10+1 = 32

The two numberings are value-complements (v → 13−v): every group of 33 becomes 65−33 = 32. Up to the solid's symmetry these are the only balances the six fives admit — a complementary pair, not a single constant.

THE SECOND SIEVE: UNAMBIGUITY

The equilibrial sieve leaves six families. Three of them are overlap covers, in which a face is shared between groups; a shared face then carries two memberships at once, an ambiguous reading. The second sieve removes every grouping with overlaps, so that each face belongs to exactly one group. Only the partitions survive.

Two sixes

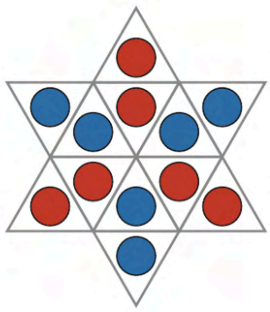

each six = 39

Three fours

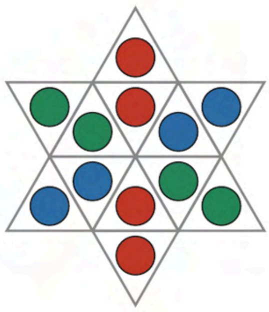

each four = 26

Six pairs

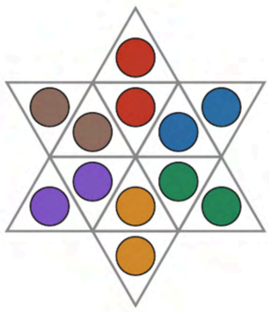

each pair = 13

Removed here, as overlap covers: six triples (which balanced at 17-22), six lines of four (26), and six fives (32/33).

Already removed by the first sieve, as unbalanceable: four triples and twelve singletons.

Three families remain, balancing at thirteen, twenty-six and thirty-nine.

The three survivors

one numbering of each, and how many such numberings exist

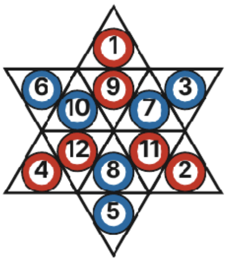

Two sixes

each six = 39

population: 30,067,200 per structure

3,126,988,800 across all placements

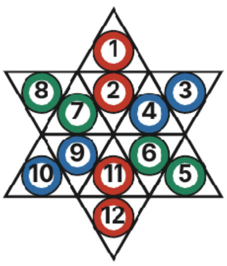

Three fours

each four = 26

population: 2,654,208 per structure

71,663,616 across all placements

Six pairs

each pair = 13

population: 46,080 per structure

460,800 across all placements

THE COMPUTATION

How the population and other numbers were computed (AI tools in plain terms)

The numberings here were not found by hand, nor by trying every possibility. They were handed to a solver, a program told the rules a numbering must obey, which then either finds one that obeys them all or proves none can. The solver is called CP-SAT; its parts, plainly:

OR-Tools

Google's free Operations Research Tools library, the optimisation toolkit the solver belongs to. (Operations research is the mathematics of the best choice under constraints.)

CP — Constraint Programming

Solving a problem by stating its variables, the values each may take, and the rules they must satisfy, then letting the program search for an assignment that satisfies every rule at once.

SAT — Boolean satisfiability

Deciding whether true/false values can be given to logical variables so a whole formula of AND, OR and NOT comes out true. (Boolean, after George Boole, means true/false logic.)

CP-SAT

The solver that rewrites a constraint-programming problem into SAT form and settles it with a SAT engine, the two above combined.

NP — nondeterministic polynomial time

The class of problems whose proposed answers can be checked quickly, even when finding one may be slow.

NP-complete

The hardest problems within NP:

a fast method for any one would give a fast method for all. SAT is one.

THE COMPUTATION (continued)

How the numbers were computed - the engine, and the proof it can give

Cook–Levin, 1971

The theorem (by Stephen Cook, and independently Leonid Levin) that SAT is NP-complete; the first problem ever shown to be so.

CDCL — conflict-driven clause learning

The search inside a modern SAT engine: each dead end becomes a new rule that prevents the same mistake twice, so very large searches still finish quickly.

CNF — conjunctive normal form

The standard shape of a SAT formula: one long AND of small OR-clauses. Rules are translated into this form before solving.

Feasible / Optimal / Infeasible

The solver's three verdicts: a solution obeying every rule exists; a provably best one is found; or a proof that no solution can exist at all.

G2P — group-to-pyramid (Grego 2 Peter)

The solid's own table saying which face of which diaquad feeds which outer-apex pyramid; it supplies the core geometry the solver must respect.

BPS — balanced permutation search

A pruned backtracking search over the numberings of the twelve values: each value is placed in turn, and the moment a group completes its sum must match the rest, or the branch is dropped. Because nothing that could still balance is ever cut, the search is exhaustive — it returns every constant a shape can reach; for the six fives, thirty-two and thirty-three.

VC — value complementation

Replacing every value v by 13−v turns a k-face group's sum S into 13k−S, so a balanced numbering stays balanced at the complementary sum — thirty-three paired with thirty-two.

THE COMPUTATION (continued)

How the numbers were computed then used here

For the four disjoint stars of the solid, the solver was given forty-eight variables, one per face, each allowed the values one to twelve. Three kinds of rule were imposed: every star must carry the twelve values once each (an all-different rule); every diaquad (a diameter's four faces) must sum to twenty-six; and every pyramid (the four faces meeting at an outer apex, one from each star) must also sum to twentysix, with the G2P table fixing which face feeds which pyramid.

Twenty-six is not a free choice

The twelve pyramid stellations of Escher's solid tile all the forty-eight faces, so if they share any sum it can only be $4 \times 78 \div 12 = 26$.

Given these rules the solver returned a numbering obeying all and confirming that such configurations exist. When the rule was strengthened (e.g. opposite faces across the centre summing to thirteen) and demanded on all eight stars, the same solver returned infeasible: not a failure to find one, but a proof that none exists.

That distinction (finding a solution versus proving none is possible) is the whole reason a SAT-based solver was used rather than a blind search through the possibilities.

The reckoning, on a small planet.
Antoine de Saint-Exupéry · The Morgan Library & Museum

RELIABILITY, THE THIRD SIEVE & THE MASKING LANDSCAPE

The third sieve asks whether a configuration is reliable: whether some numbering makes all twelve outer-apex pyramids, the *pyraquads*, sum alike — necessarily to twenty-six, since the twelve pyramids tile all forty-eight faces and 12 × 26 = 4 × 78.

Equilibrium kept what could balance; unambiguity kept what reads only one way; reliability asks what can be read on the solid's twelve readings all at once.

The working scope is the four disjoint stars: A, B, C and D, one value-partition each. Counted up to the solid's symmetry they number C(35, 4) = 52,360 combinations: the 8,366 with all twelve diaquads distinct, together with 43,994 that repeat a diaquad.

Each reliable numbering has a shape. When two or more pyramids carry the same four values they coincide in a block, a mask, a place where a rare reading can hide behind a look-alike (a 'zebra').

A pyramid whose quadruple is unique is a clear, distinct reading (a 'horse'). A shape records how many of the blocks are pairs, triples and quads. Two bounds hold, both proven. Ceiling: every value sits on exactly four of the forty-eight faces, so no reading is masked more than four-fold, and four is reached. Floor: the twelve pyramids never collapse below five distinct readings. The deepest fold, the (4,0,1) singularity, is reached once up to the solid's symmetry.

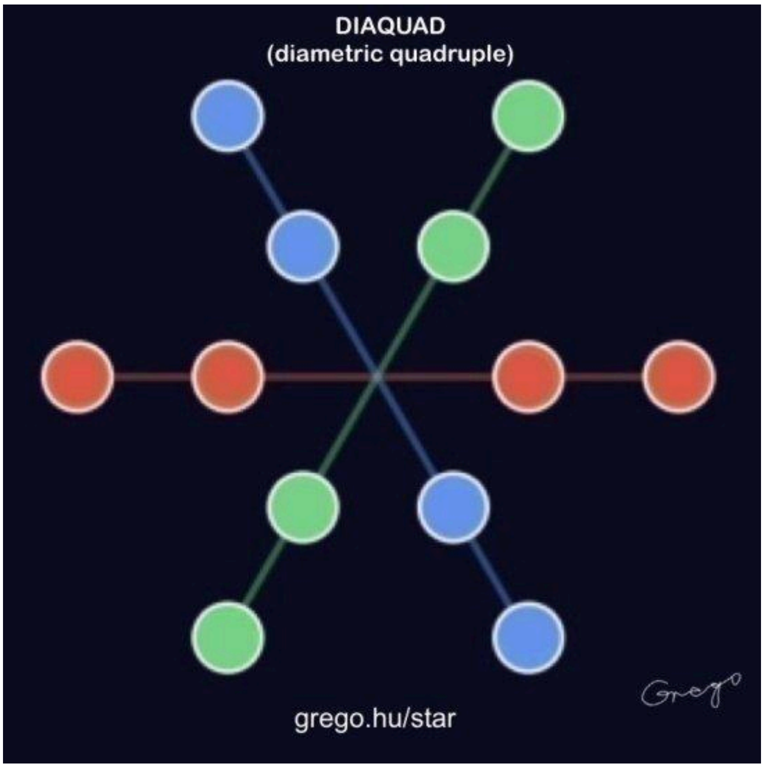

The Diaquad — three diametric quadruples, each summing to 26

SOME STRUCTURAL LAWS

Proven across the landscape

Ceiling — no mask beyond four

Each value lies on four faces, so a quadruple shared by N pyramids needs N copies of each value: $N \leq 4$. Five- and six-fold masks are impossible; the four-fold maximum is reached.

A clear reading exists for every combination but one

(See the ALBINO STAR model on grego.hu/star) Every diaquad-magic combination admits a fully unique, “all-horses” reading on pyraquads except #4366 = [5,8,17,21]*, whose pyramids never all read apart, the albino end. * star-face combination IDs, not sum values.

The lone quad is rare, not impossible

A single four-fold mask among eight clear pyraquad readings does occur, on exactly three combinations: [1,16,20,26], [1,16,20,29] and [7,11,17,18]. Once thought forbidden, merely scarce.

No five-pair gap

The five-masked-pair shape (5,0,0), in the notation for identical pyraquads (pair, triple, quadruple), is not absent; it occurs nine times across the symmetry-respecting census. There is no gap at ten masked pyramids.

Floor — five distinct readings

The twelve pyramids never collapse below five distinct readings. The deepest fold, the (4,0,1) shape (four masked pairs and one quad, no unmasked read left), is that floor, reached exactly once up to the solid’s symmetry: THE SINGULARITY, an absolute goal of the present model and research, successfully proven.

Symmetry governs collapse

Heavy folding needs a symmetric combination: the more alike the four magic stars, the further the herd folds. The Quadruplet calculations attest, there the four disjoint stars are not distinct (see Summetry Summit - the litmus test of the model, from page 62), dramatically changing the landscape.

Sieved by the principles of summetry, the Diaquads (along with its chiral twin cousins, the two Z-quad shapes, see pages 63–66) **are the only survivors and their achiral shape becomes the absolute top-of-the-podium finalist to further study, due to its equilibrally balanced, unambiguous and reliable stability, corresponding to the vector equilibrial core architecture of Escher’s solid** (see the “Apple - cuboctahedron - invagination” animation on the grego.hu/star).

THE SINGULARITY

The singular end, the outcast, the common ones — and the stars you can orbit

The three-tier Escher-Grego Polyhedral Sieve Model for Medical Diagnostics downgrades the parameter population multitudes from the space-filling solid’s 48-face factorial numbering that’s well over the number of atoms in the entire Solar System to those of an approximately one-month-old human Embryo, while incorporating key anatomic and biological correlations through the adaptation of high-fidelity scales, all through the principle of *summetry*, the discrete geometric-arithmetic unity of symmetry and combinatorics.

The goal: a model for sieving the zebra(s) when there are only hoofbeats heard - as the paraphrased teaching originally attributed to Prof. Dr. Theodore E. Woodward (USA) goes.

Based on solid clinical experience, the aphorism’s wisdom is also a prudent warning for ambitious young medics who often tend to pride and prize themselves by pinpointing rare conditions learnt in class, a manifestation of the common availability heuristic fallacy (if it comes to mind easily, it must be realistically probable). Not in the present study, I sincerely hope.

The goal is achieved here by the meticulous application of highly sophisticated and custom made calculations that are themselves a form of carefully balanced sieves, ensuring that existing and real data-processing capacity limitations do not force the author to compromise the strict numeric hierarchies involved, but rather, allow for the clear formulation of conjectures that could thus be proven theorems.

The sought singularities have been reached and the landscape of masked zebras has been fully explored and demonstrated.

THE SINGULARITY (continued)

At one end of the modeled spectrum, we present the lone and unique occurrence of the “(4,0,1)” Star Face, the Phantom Star (4 pairs, zero triples and 1 quadruple of identical pyramid readings) that opens the way to look for zebras only, in hope of a clear and confirmable, or even an immediate diagnosis, where the symptom-diagnosis-therapy triad can suddenly fold into a single, almost holistic sequence, much like the equilibrium-unambiguity-reliability sieve itself.

At the other end, we show that there is another singular instance (that of the #4,366 combo of four 2D star faces) when no clear diagnosis is possible by the 3D model, as the outer pyramid-quadruples never admit an all unique reading, clear or even contrasting test results and thus firm diagnoses are ruled out – zebras never have stripes and horses are never brown or black, it is like the “albino among the vitiligo testing patients”. Another perfect call for an *ex juvantibus* therapy, especially during ER treatment or other life-threatening situations.

The shareable STAR FACE landing card — the four orbitable stars live at grego.hu/star

THE SINGULARITY (continued)

In contrast, a BRIGHT STAR is also presented on the grego.hu/star page; it is a ~56% occurrence, all pyramids unique, all add up to the magic 26 sum just like the diametric quadruples (diaquads) of the four disjoint magic hexagrams: luckily, a majority of cases fall in this category where examinations, test results and anamnestic data are all in sync to ground a true and certain *Vera certissima* diagnostic verdict. A strong indication not to look for a zebra while hearing the hoofbeats.

Finally, to illustrate another quite frequent (~33%) challenge in medical diagnostics, the enumerated and manually orbitable MASKED STAR model, the “(1,0,0) case” yielding a single pair of non-distinct pyramids representing a camouflaged zebra among the horses, is also animated on the interactive demonstration page.

Easy to miss, this “masked zebra” may itself be the epitome of the entire polyhedron model and only the experienced physician will be able to confirm whether the sieve presented here offers a frequency result that correlates to real-life experience or not.

If yes, this would highlight an important explanation for the vicious cycle of the rare disorder phenomenon: masked, misdiagnosed or merely mitigated, in the absence of a timely diagnosis the disease quietly takes its toll on the patient’s health — in stealth. Like dense crops covering a hare, records mark the disease as “rare”.

NORD®
National Organization for Rare Disorders

The author’s (no affiliation) recommendation for readers: founded in 1983, NORD® continues to be a “full-service, mission-driven, and independent nonprofit reimagining a future where every person with a rare disease and their families live their best lives”.

THE FULL CENSUS

Every reading-shape across all 6,223,974 pyramid-magic numberings

Counted up to the symmetry of the solid, the four disjoint stars admit 8,366 diaquad-magic combinations and 6,223,974 pyramid-magic numberings. Of these, 3,538,104 are fully distinct (every pyramid a clear read), and exactly one combination, #4366, admits none. No reading is ever masked more than fourfold (the ceiling), and the twelve pyramids never fall below five distinct reads (the floor).

shape	reading-shape	distinct reads	numberings	share
(0,0,0)	**all clear**	**12**	**3,538,104**	**56.85 %**
(1,0,0)	**one pair**	**11**	**2,079,465**	**33.41 %**
(2,0,0)	**two pairs**	**10**	**505,208**	**8.12 %**
(3,0,0)	**three pairs**	9	56,916	0.91 %
(4,0,0)	**four pairs**	8	3,013	0.048 %
(5,0,0)	**five pairs**	7	9	0.0001 %
(6,0,0)	**six pairs**	6	91	0.0015 %
(0,1,0)	**one triple**	10	21,287	0.342 %
(1,1,0)	**pair + triple**	9	14,982	0.241 %
(2,1,0)	**two pairs + triple**	8	4,132	0.066 %
(3,1,0)	**three pairs + triple**	7	160	0.0026 %
(0,2,0)	**two triples**	8	198	0.0032 %
(1,2,0)	**pair + two triples**	7	314	0.0050 %
(0,3,0)	**three triples**	6	78	0.0013 %
(0,0,1)	**lone quad**	9	3	< 0.001 %
(1,0,1)	**pair + quad**	8	8	0.0001 %
(2,0,1)	**two pairs + quad**	7	3	< 0.001 %
(4,0,1)	**four pairs + quad**	**5 (lowest)**	**1 (singularity)**	**< 0.001 %**
(1,1,1)	**pair + triple + quad**	6	2	< 0.001 %

Grego’s Polyhedral Sieve Model for Medical Diagnostics — The Full Census, 2026

Shape = (pairs, triples, quads): blocks of pyramids that share one four-value reading.
Shares are assign-weighted across all **6,223,974** numberings.

The masking landscape

clock of the twelve pyramids — all clear — (0,0,0)

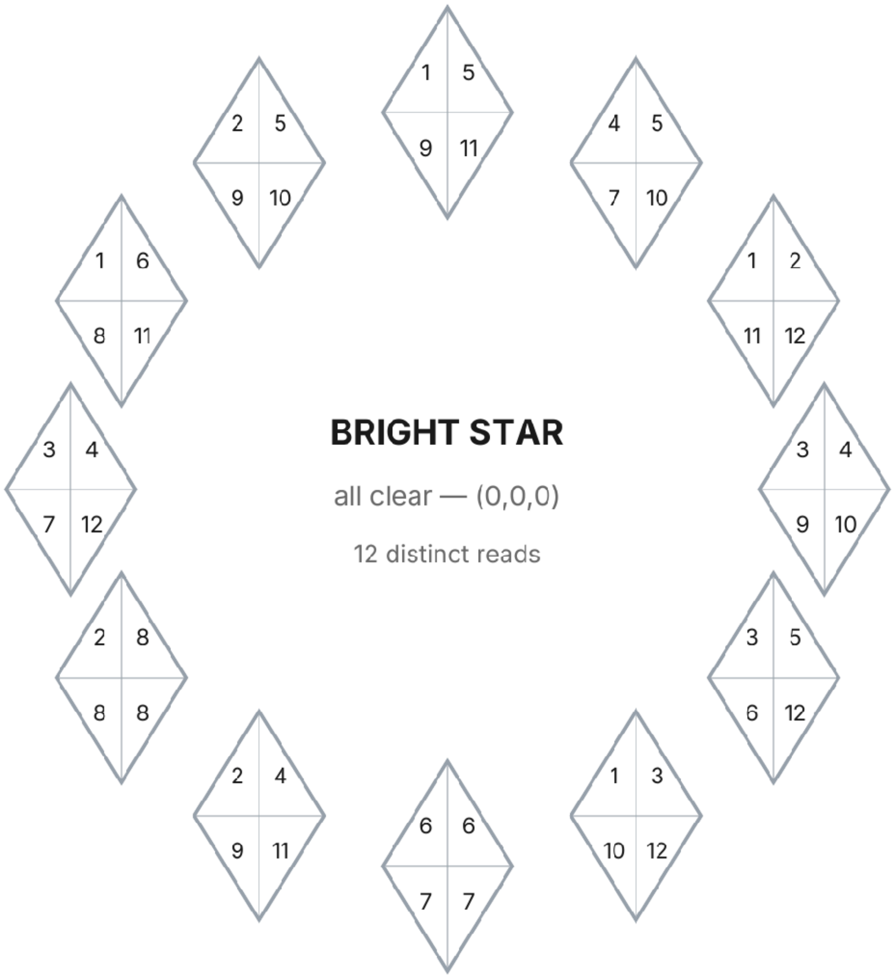

THE COMMON CASE — 56.85%

every pyramid a clear, distinct read — no zebra can hide

3,538,104 of 6,223,974 numberings

Shape (0,0,0) — see The full census table.

Interactive 3D BRIGHT STAR Escher's solid model: grego.hu/star

The masking landscape

clock of the twelve pyramids — one pair — (1,0,0)

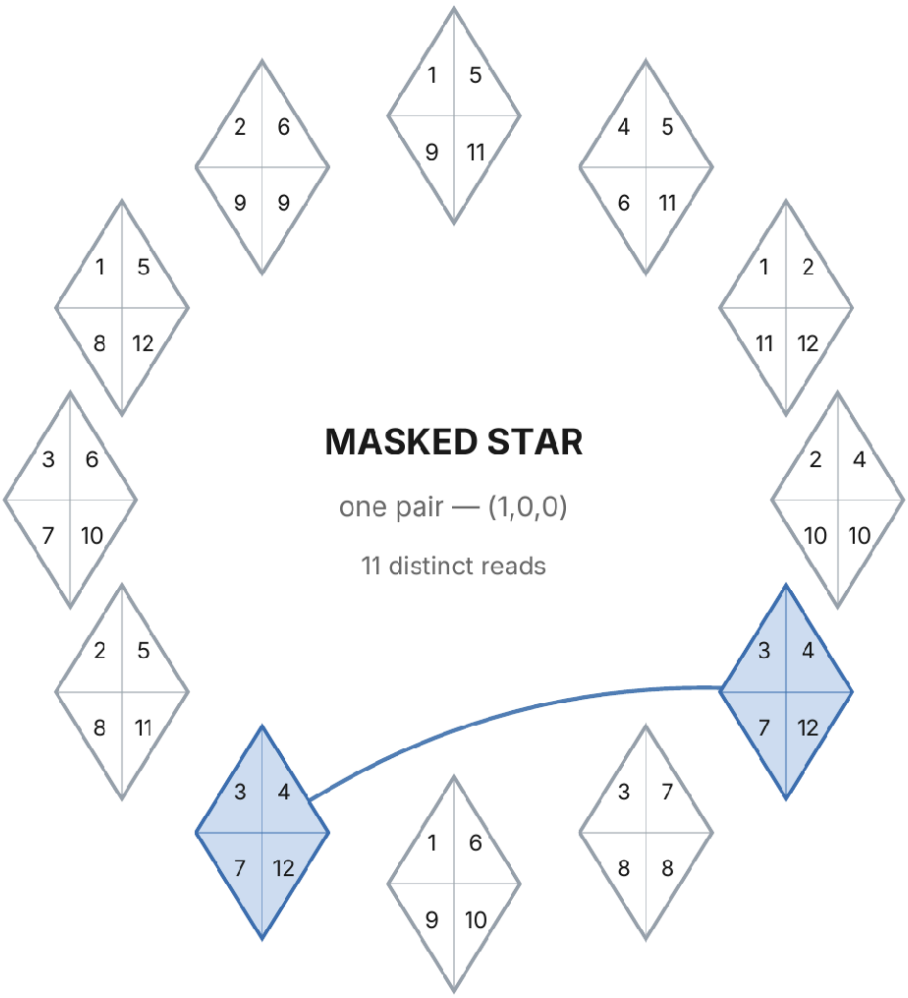

THE COMMON CHALLENGE — 33.41%

two reads merge — one place a zebra could hide

2,079,465 of 6,223,974 numberings

Shape (1,0,0) — see The full census table.

Interactive 3D MASKED STAR Escher’s solid model: grego.hu/star

The masking landscape

clock of the twelve pyramids — two pairs — (2,0,0)

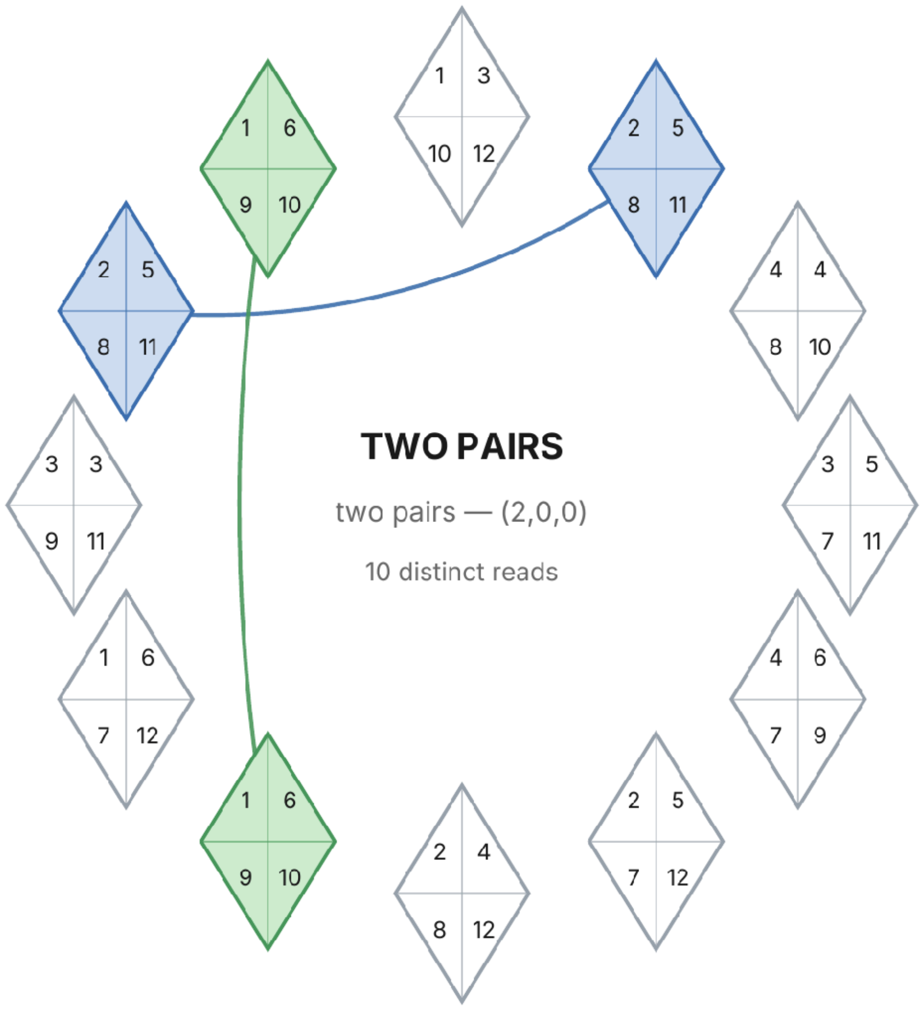

MASKING DEEPENS — 8.12%

two coincidences among ten clear reads

505,208 of 6,223,974 numberings

Shape (2,0,0) — see The full census table.

Orbit the four magic stars in 3D: grego.hu/star

The masking landscape

clock of the twelve pyramids — three pairs — (3,0,0)

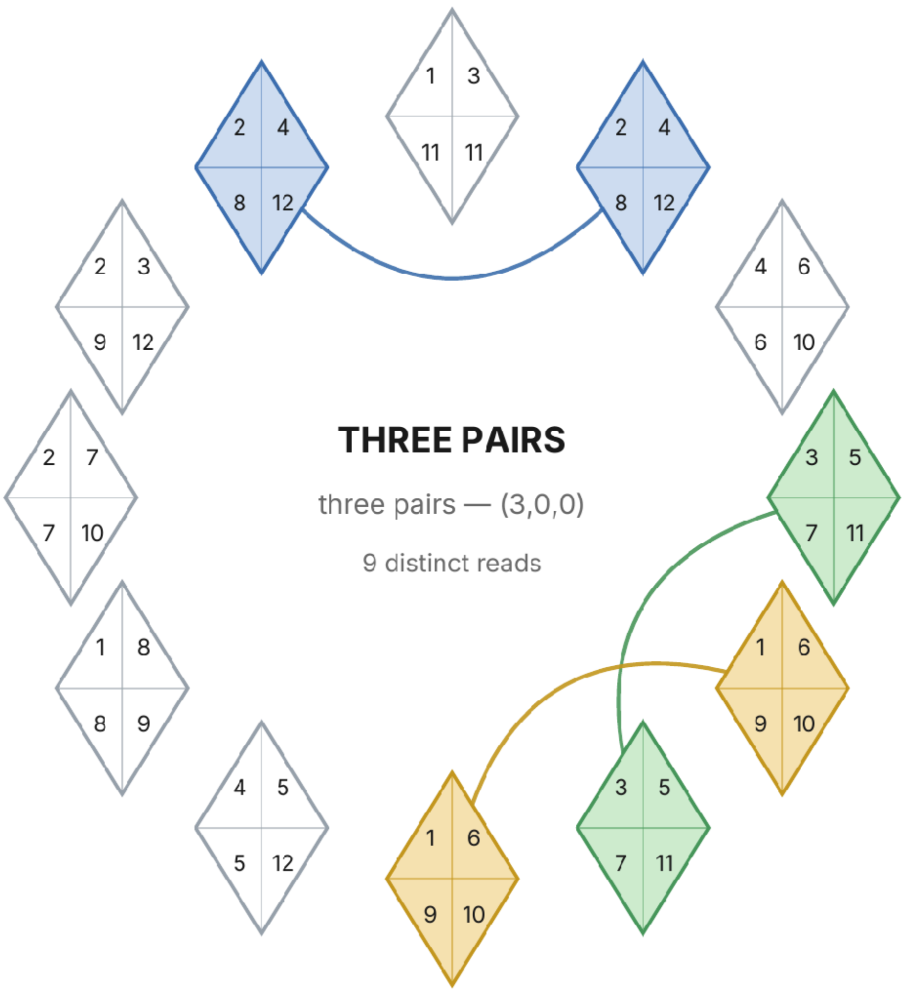

RARER STILL — 0.91%

three coincidences; six reads still clear

56,916 of 6,223,974 numberings

Shape (3,0,0) — see The full census table.

Orbit the four magic stars in 3D: grego.hu/star

The masking landscape

clock of the twelve pyramids — five pairs — (5,0,0)

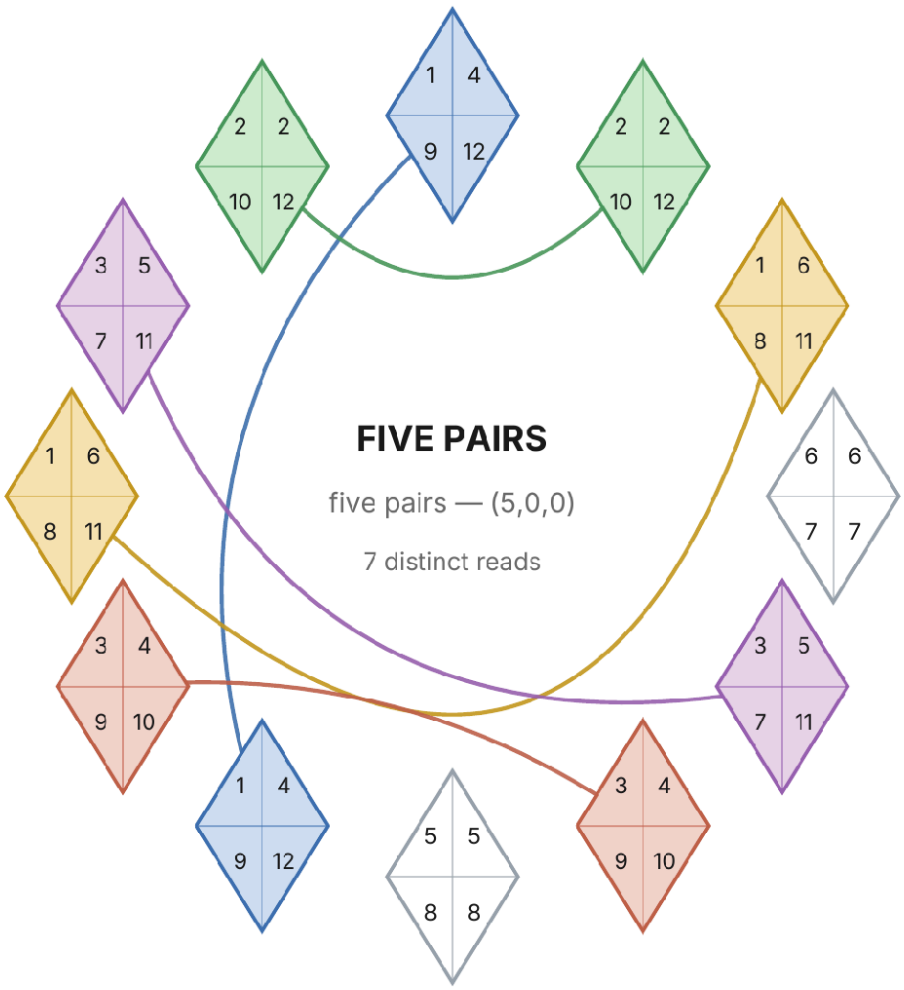

NO GAP — IT DOES OCCUR

once thought impossible; the five-pair shape does appear

9 of 6,223,974 numberings

Shape (5,0,0) — see The full census table.

Orbit the four magic stars in 3D: grego.hu/star

The masking landscape

clock of the twelve pyramids — lone quad — (0,0,1)

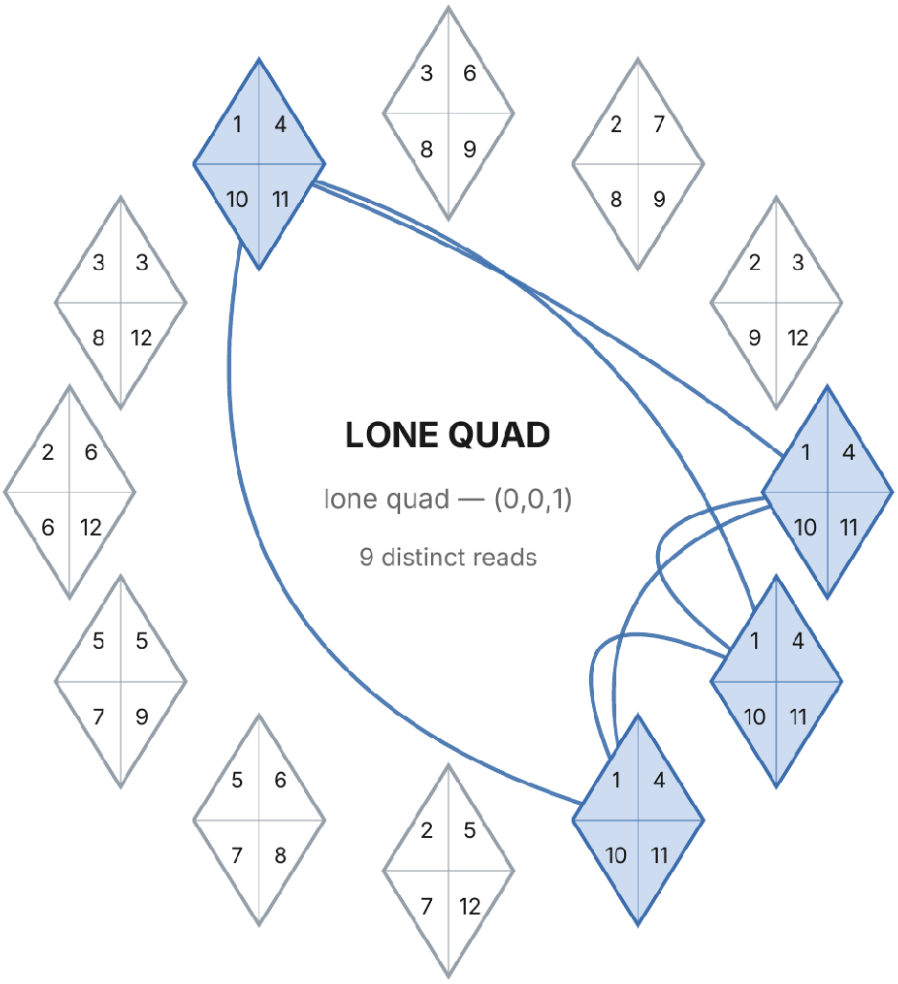

RARE, NOT IMPOSSIBLE

a single fourfold mask among eight otherwise-clear reads

3 of 6,223,974 numberings

Shape (0,0,1) — see The full census table.

Orbit the four magic stars in 3D: grego.hu/star

The masking landscape

clock of the twelve pyramids — the (4,0,1) singularity

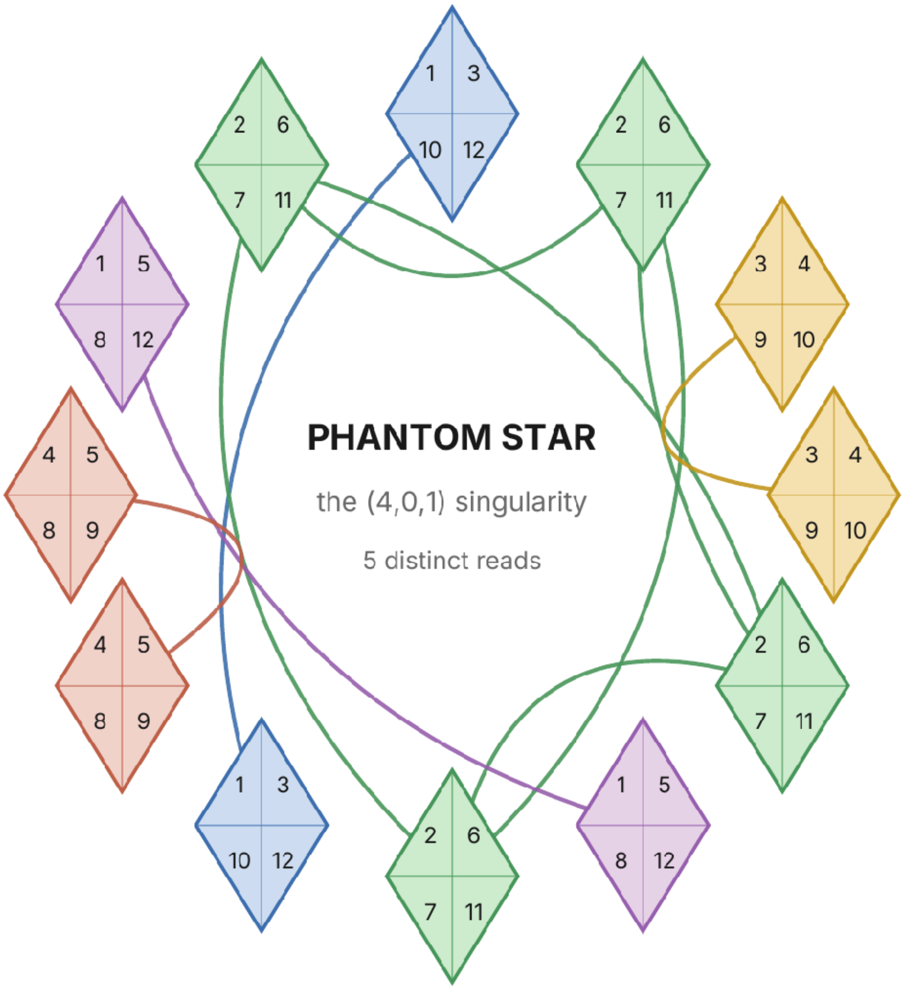

THE SINGULARITY — occurs once

the floor: one fourfold mask and four masked pairs, no unmasked read left

1 of 6,223,974 numberings, unique up to the symmetry of the solid

Shape (4,0,1) — see The full census table.

Interactive 3D PHANTOM STAR Escher's solid model: grego.hu/star

The masking landscape

clock of the twelve pyramids — the #4,366 exception — (0,2,0)

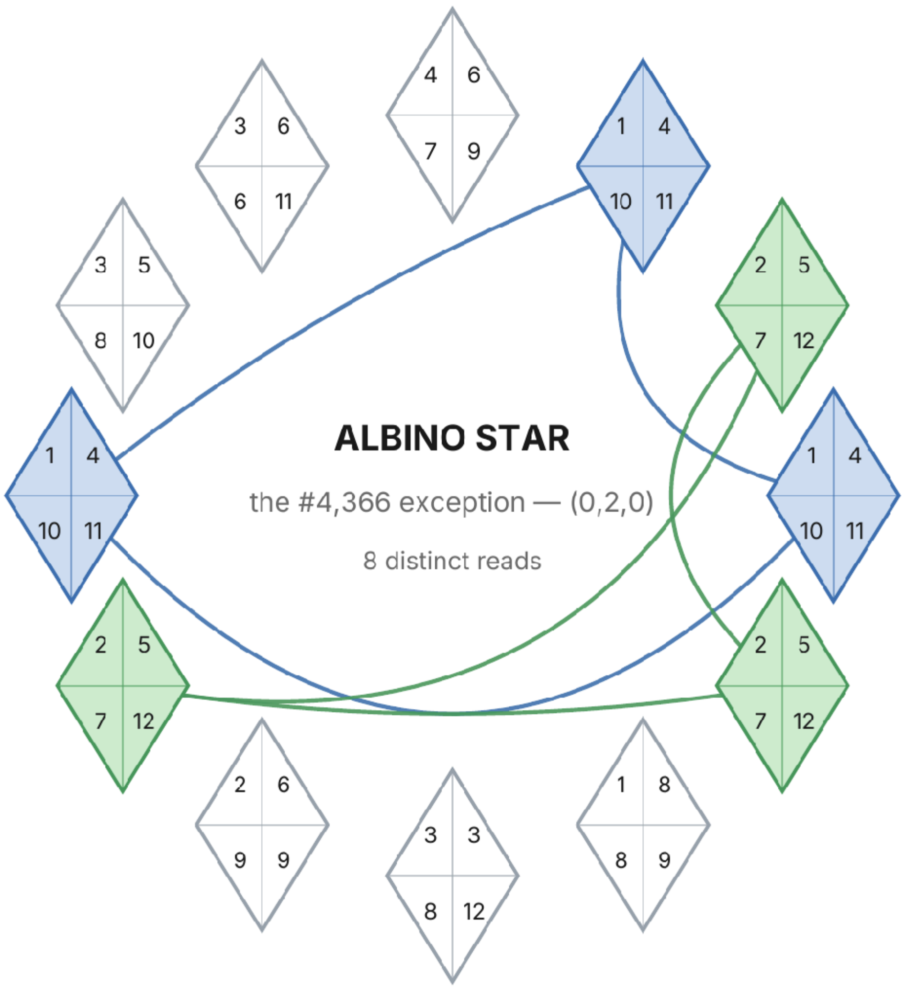

THE EXCEPTION — no all-distinct reading exists

the only combination whose pyramids never all read apart

combination #4366 = [5,8,17,21]

Shape (0,2,0) — see The full census table.

Interactive 3D ALBINO STAR Escher's solid model: grego.hu/star

FRONTIER DIAGNOSTICS BEHIND THE PYRAMIDS

THE NEXT ROSTER, STILL IN THE LABORATORY

Each four-faced pyramid stands, in the model, for one reading the clinician orders, and the readings are changing. What follows surveys diagnostic tools still in research and development, not yet finalised, that will fill those slots. Sources are numbered and listed under References. They are grouped by what they read.

Molecular and omic readouts

Multi-cancer early detection (MCED) liquid biopsy

One blood draw read for tumour-DNA methylation and fragments to flag fifty-plus cancers, often before symptoms; Galleri reports ~51% sensitivity at ~99.5% specificity. Not yet a finalised screen. [R4]

CRISPR diagnostics (SHERLOCK / DETECTR)

Cas13 and Cas12 detect pathogen nucleic acids at attomolar levels in under an hour, with lateral-flow point-of-care readout; multiplexing matures and an FDA submission is underway. [R5]

Plasma proteomics at scale

Affinity platforms read thousands of plasma proteins from a small sample (SomaScan ~11,000, Olink Explore HT ~5,400), feeding risk panels still being standardised. [R7]

Chemistry in motion; energy, field and structure

Chemistry in motion

Breath analysis / electronic nose

Exhaled breath carries over a thousand volatile compounds; sensor-array ‘e-noses’ with machine learning read their fingerprints for cancer, respiratory and metabolic disease. [R6]

Wearable continuous multiplexed biosensors

Skin sensors sample sweat or interstitial fluid for many analytes at once (glucose, lactate, cortisol, urea, drugs) continuously; a 2026 regenerable patch ran for twenty-one days. [R8]

Energy, field and structure

Photon-counting CT (PCCT)

Detectors that count individual X-ray photons: ultrahigh resolution at much lower dose, with intrinsic spectral data. High-end only; a portable extremity unit was FDA-cleared in 2026. [R1]

Total-body PET (uEXPLORER class)

A ~194 cm detector images the whole body at once with a 30-40x sensitivity gain, enabling ultra-low dose and dynamic kinetics. A handful of systems exist worldwide. [R2]

Chemistry in motion; energy, field and structure (cont.)

Hyperpolarised 13C metabolic MRI

Injected polarised pyruvate is watched turning into lactate in real time, imaging metabolism and treatment response earlier than standard MRI. A few research scanners. [R3]

Magnetocardiography (OPM-MCG)

Optically-pumped quantum magnetometers map the heart's femtotesla field contactfree; rest MCG outperforms rest and even stress ECG for ischemia. Standardisation is the open step. [R9]

Optoacoustic / photoacoustic imaging

Laser pulses make tissue emit ultrasound, joining optical molecular contrast (oxygenation, vasculature) to ultrasound depth; in cancer and vascular trials. [R10]

Ultrasound localization microscopy (ULM)

Localising single microbubbles across frames beats the acoustic diffraction limit, mapping micron-scale vessels deep in tissue; in-human feasibility has been shown. [R11]

Oculomics

AI reads the retina (fundus, OCT, angiography) as a window on cardiovascular, neurological, renal and metabolic disease from a non-invasive scan. [R12]

THE INTERPRETATIVE LAYER, AND THE SUCCESSION

The interpretive layer

Medical foundation models (multimodal AI)

Generalist models trained across images, text, signals, genomics and pathology act as the integrating reader that turns many separate readouts into a single assessment. [R13]

Succession — how the new roster replaces the old

Under ideal future conditions diagnosis shifts along seven axes: i) invasive to non-invasive, ii) episodic to continuous, iii) anatomical to molecular and functional, iv) single-analyte to multiplexed, v) reactive to predictive, vi) centralised to point-of-care, vii) human-read to AI-integrated.

The older single-purpose tools do not merely improve; they become redundant once a cheaper, richer, continuous reader covers the role.

Established tool	Frontier replacement
Blood-pressure cuff	continuous cuffless / multiplexed wearables
ECG / EKG	magnetocardiography + continuous wearable ECG
Lab blood panels	plasma proteomics + on-body biochemistry + CRISPR
Plain X-ray	low-dose photon-counting CT; super-res ultrasound
Conventional CT	photon-counting CT
Ultrasound	ultrasound localization microscopy + optoacoustic
MRI	hyperpolarised metabolic MRI; fast AI / portable MRI
PET / CT	total-body PET
Targeted genetic panels	rapid whole-genome / nanopore + CRISPR
Tissue biopsy	liquid biopsy + imaging virtual biopsy
Periodic screening visits	oculomics + breath + passive wearables
Human-only interpretation	multimodal foundation models

A DISTRIBUTION ACROSS PYRAMIDS OF ESCHER'S SOLID

One novel diagnostic per pyramid; the AI model binds them

The medical foundation model is not a thirteenth pyramid; it is the binding constant, the reader that sums the twelve readouts into one diagnosis, **the clinical analogue of the magic sum.**

Pyramid	Novel diagnostic	reads
P1	MCED liquid biopsy	circulating tumour DNA
P2	CRISPR point-of-care	pathogen nucleic acids
P3	Plasma proteomics	thousands of proteins
P4	Breath / electronic nose	volatile fingerprints
P5	Wearable biosensors	sweat & ISF chemistry
P6	Photon-counting CT	spectral structure, low dose
P7	Total-body PET	whole-body kinetics
P8	Hyperpolarised 13C MRI	live metabolism
P9	Magnetocardiography	cardiac magnetic field
P10	Optoacoustic imaging	oxygenation, vasculature
P11	Ultrasound loc. microscopy	micron-scale vessels
P12	Oculomics	retina as systemic marker

Bind — Medical foundation AI model — integrates all twelve.

Dudeney’s ceiling, and the diaquad star

a supercomputer search of the magic-star numberings

Dudeney’s magic star numbers the six lines of the hexagram so that each line of four sums to twenty-six. Carried onto the solid (the twelve faces of each star numbered in this classical way across the four disjoint stars), a sharper question follows: how many of the twelve pyramids, the quadruples meeting at the outer apexes, can be made magic at once, each summing to twenty-six? By hand, four was the most that could be coaxed out; the form seemed to resist more.

To settle it, the body-numberings were enumerated exhaustively. Each disjoint star admits 960 Dudeney-valid tables; across the four stars that is 960^4, some 849 billion numberings of the whole solid. The search was joint work with Gergő Kiss, run on the HUN-REN Cloud (a 32-CPU instance) over four days and eight hours. The verdict is exact: the greatest number of magic pyramids any Dudeney numbering attains is ten, reached by exactly 144 numberings. Eleven and twelve never occur.

Magic pyramids	Body-numberings
0	404,124,906,186
1	310,052,121,672
2	108,548,849,364
3	22,968,740,688
4	3,287,272,920
5	337,211,016
6	25,822,116
7	1,550,472
8	81,462
9	3,960
10	**144**
11	0
12	0

The twelve counts sum to 849,346,560,000 = 960^4 — the whole space, accounted for.

the first ten-pyramid numbering, and what it confirms

First numbering with ten magic pyramids (plate code 1·694·823·52),
the four disjoint stars K, C, M, Y across positions one to twelve:

K	7	9	1	2	8	11	12	3	4	5	6	10
C	10	11	7	1	4	12	6	8	2	9	3	5
M	4	5	3	10	7	2	11	8	9	1	6	12
Y	12	2	9	4	8	6	7	11	1	3	5	10

When the further constraint is imposed that the outer David-star triangles also sum to twenty-six, the ceiling falls to eight, met by 48 numberings, and never higher.

This is the supercomputer's confirmation of the sieves. Dudeney's constellation, however it is numbered, can never make the solid fully reliable: some pyramids must always disagree. Ten is the proven ceiling; twelve is forever out of reach. The unambiguity and reliability sieves are vindicated not by argument alone but by exhaustive count.

Gergő Kiss, Dániel Erdély, Grego
Budapest, February, 2024 (photo: Ottó István Mészáros)

THE DIAQUAD STAR

The same result throws the alternative into relief. Where Dudeney's classical numbering cannot reach twelve, another numbering does, and does so by symmetry rather than by search.

The diaquad (the diagonal quadruple) numbers the twelve faces directly, in three groups of four. Each group lies along the diagonals of one of the solid's three principal symmetry planes, the planes parallel to its faces; the three planes give the three diaquads, and the numbering simply follows their diagonals. The mapping is shown in motion in the animation at grego.hu/star. Because the figure's own symmetry carries the balance, the pyramids sum to twenty-six by construction, with no number used twice. This is the SUMMETRY: a magic earned from the symmetry of the form, not imposed upon it.

So the supercomputer does two things at once. It closes the classical question (Dudeney's star has a ceiling of ten) and it certifies the new one: the diaquad numbering is a genuine, valid magic star, exact precisely where the older construction falls short.

A large-scale supercomputer search has confirmed the unambiguity sieve's verdict: Dudeney's magic-star constellation can never make all twelve of the pyramids magic at once, so the solid admits at most ten magic pyramids.

With special thanks to Dániel Erdély and Gergő Kiss, to Lajos Szilassi, and to the HUN-REN Cloud Team at Wigner Research Centre for Physics.

SUMMETRY SUMMIT — THE MODEL'S LITMUS TEST

Chirality, census constraints & clinical comparisons

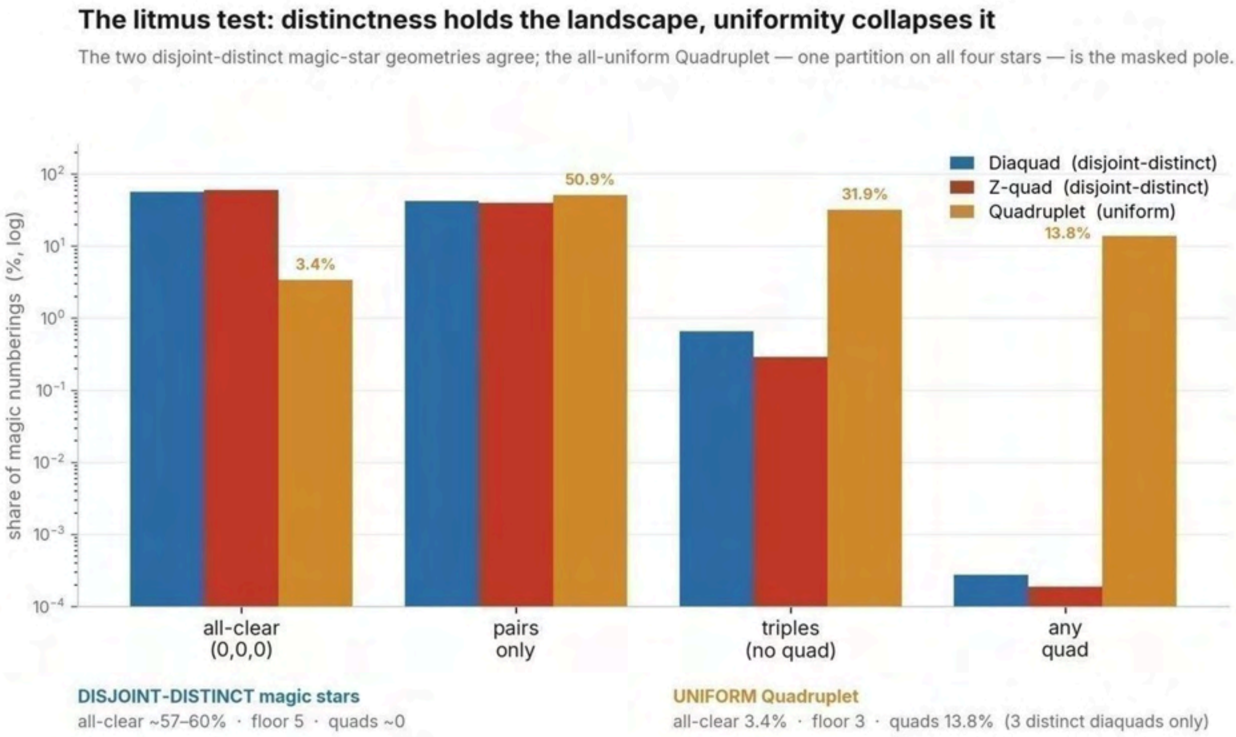

Masking landscape — three readings of the solid

	Diaquad	Z-quad	Quadruplet
all-clear (0,0,0)	56.85%	59.78%	3.39%
pairs only	42.49%	39.93%	50.88%
triples (no quad)	0.661%	0.291%	31.93%
any quad	0.0003%	0.0002%	13.81%
total magic	6,223,974	8,012,836	473,744
floor / ceiling	5 / ≤4	5 / ≤4	3 / ≤4

Shares of pyramid-magic numberings (assign units). **D** & **Z** = the disjoint-distinct magic stars (8,366 combos); Quadruplet = one partition on all four stars.

Difference from the diaquad (percentage points)

	Z-quad − Diaquad	Quadruplet − Diaquad
all-clear	+2.93	−53.46
pairs only	−2.56	+8.39
triples	−0.37	+31.27
any quad	≈ 0	+13.81

Exact, exhaustive counts — no sampling error.
Z-quad sits within a ≤2.9-point band of the diaquad (invariant). The Quadruplet departs by 8–53 points — a different regime, not a wobble.

My summetry conjecture, now confirmed towards a Summetry Sieve Theorem, was that consistently applying a purely logical and maximally symmetry-respecting sieve using a string of carefully selected constraints would reduce the astronomic combinatorial census (probabilities) into a fair, undistorted and realistic one which always admits a solid-numbering yielding 2D magic (sum 26) in 3D, while keeping the variance of the analyzed masking landscape undistorted, within a reasonable statistical margin of error: finding the zebra despite the hoofbeats (→ diagnosis).

The mirror test: Diaquad versus Z-quad

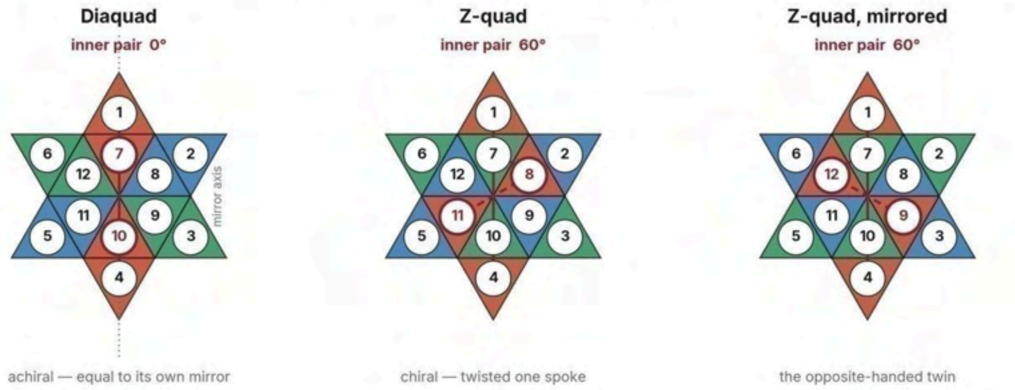

The diaquad is invariant under every symmetry of the star, so a reflection returns the same figure.
Z-quad's inner pair is rotated one spoke (60°); a reflection carries it to a distinct twin.
The red group's tip axis (solid) and inner-pair axis (dashed) show the twist.

To confirm this, three full censuses and masking landscapes were calculated and readied for numeric and graphic juxtaposition (see tables and graphs below); first, relaxing the Diaquad's strict achiral invariance constraint (→ Z-quad), then, removing the distinct partition constraint imposed on the 12 quadruples of the 3D solid's four disjoined magic stars (→ Quadruplet), as well.

The full masking landscape — all three readings

Shape (P,T,Q): a pair / triple / quad = 2 / 3 / 4 pyramids reading the same number-set; every other pyramid reads uniquely. Exact assign-unit counts; — = shape absent.

		Diaquad		Z-quad		Quadruplet	
(P,T,Q)	**what shares a read**	count	%	count	%	count	%
(0,0,0)	all distinct	3,538,104	56.85	4,790,116	59.78	16,036	3.38
(1,0,0)	1 pair	2,079,465	33.41	2,585,376	32.27	43,248	9.13
(2,0,0)	2 pairs	505,208	8.12	553,714	6.91	75,716	15.98
(3,0,0)	3 pairs	56,916	0.914	56,895	0.710	66,208	13.98
(4,0,0)	4 pairs	3,013	0.048	3,314	0.041	36,032	7.61
(5,0,0)	5 pairs	9	0.00014	10	0.00012	—	—
(6,0,0)	6 pairs	91	0.0015	97	0.0012	19,840	4.19
(0,1,0)	1 triple	21,287	0.342	12,802	0.160	4,880	1.03
(1,1,0)	pair + triple	14,982	0.241	8,253	0.103	12,480	2.63
(2,1,0)	2 pairs + triple	4,132	0.066	1,984	0.025	55,176	11.65
(3,1,0)	3 pairs + triple	160	0.0026	46	0.00057	34,720	7.33
(0,2,0)	2 triples	198	0.0032	100	0.0012	480	0.101
(1,2,0)	pair + 2 triples	314	0.0050	103	0.0013	22,912	4.84
(0,3,0)	3 triples	78	0.0013	11	0.00014	20,608	4.35
(0,0,1)	1 quad	3	0.00005	1	0.00001	—	—
(1,0,1)	pair + quad	8	0.00013	2	0.00002	128	0.027
(2,0,1)	2 pairs + quad	3	0.00005	7	0.00009	6,880	1.45
(4,0,1)	4 pairs + quad	1	0.00002	1	0.00001	20,640	4.36
(1,1,1)	pair + triple + quad	2	0.00003	—	—	1,536	0.324
(0,2,1)	2 triples + quad	—	—	4	0.00005	21,504	4.54
(0,0,3)	3 quads	—	—	—	—	14,720	3.11
total	floor / ceiling →	**6,223,974**	5/≤4	**8,012,836**	5/≤4	**473,744**	3/≤4

Diaquad and Z-quad are the disjoint-distinct magic stars (floor 5, ceiling ≤4); the uniform Quadruplet drops to floor 3.
Named shapes: (0,0,0) bright · (5,0,0) five-pair · (0,0,1) lone quad · (4,0,1) singularity / floor · (0,0,3) three quads.

CHIRALITY

While Nature uses chirality on a molecular level to create complex, information-rich structures starting from DNA and enzymes all the way to our inner anatomy, achirality is observed when achieving balance, structural simplicity and physical neutrality against the unbiased laws of physics and gravity is necessitated, including on our outer body organs and limbs.

Planets gravitate (→ achirality), while the Embryo develops strictly clockwise (heart on the left, liver on the right → chirality). One of the main, simple reasons behind the existence of life on Earth is that water neither evaporates, nor freezes: like Escher's solid, water molecules are achiral, providing stability in an unbiased physical state through equilibrium, unambiguity and reliability: exactly the three sieves used in the model.

Interestingly, bodies of most living creatures, like us, humans, too, are highly chiral internally, yet appear achiral on the outside, and there is a strong reason for that: a truly chiral overall arrangement of outer organs would be inefficient against threats, but achirality ensures physical stability, movement and optimal survival skills.

Its achirality-coded invariance is exactly the reason why the Diaquad survived the third and final reliability sieve on the 8,366 combos of the solid's four disjoint-distinct magic stars: Diaquad's chiral cousin, the Z-quad (seen second from left in the bottom row on page 11, {1,4,8,11}) finished in a quasi near dead heat, though, producing an almost identical masking landscape, albeit on a larger census.

An imagined scene illustrating the difference between the Diaquad and the two Z-quads follows:

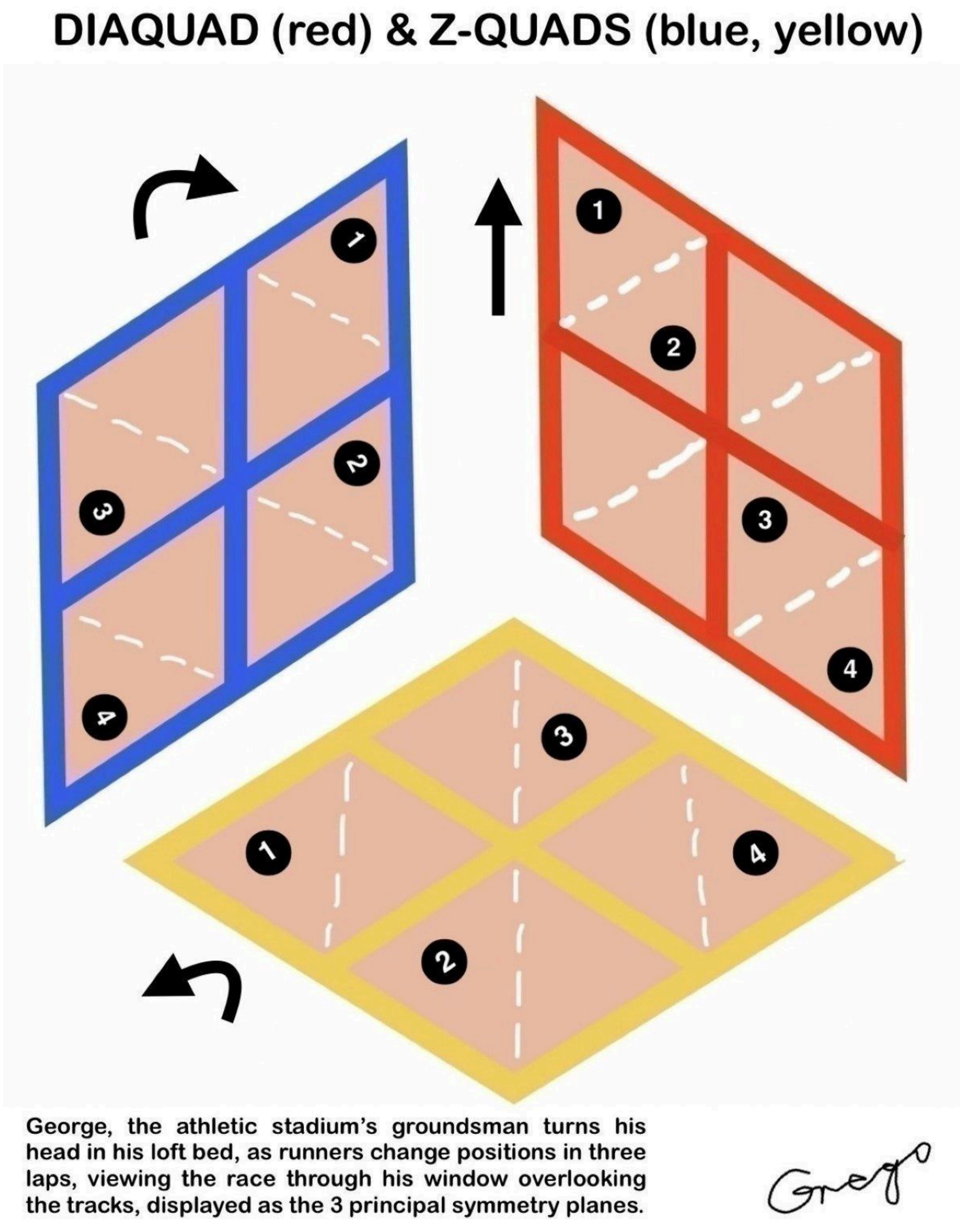

George, the athletic stadium's groundsman turns his head in his loft bed, as runners change positions in three laps, viewing the race through his window overlooking the tracks, displayed as the 3 principal symmetry planes.

Related: the Race Outcome Formula:

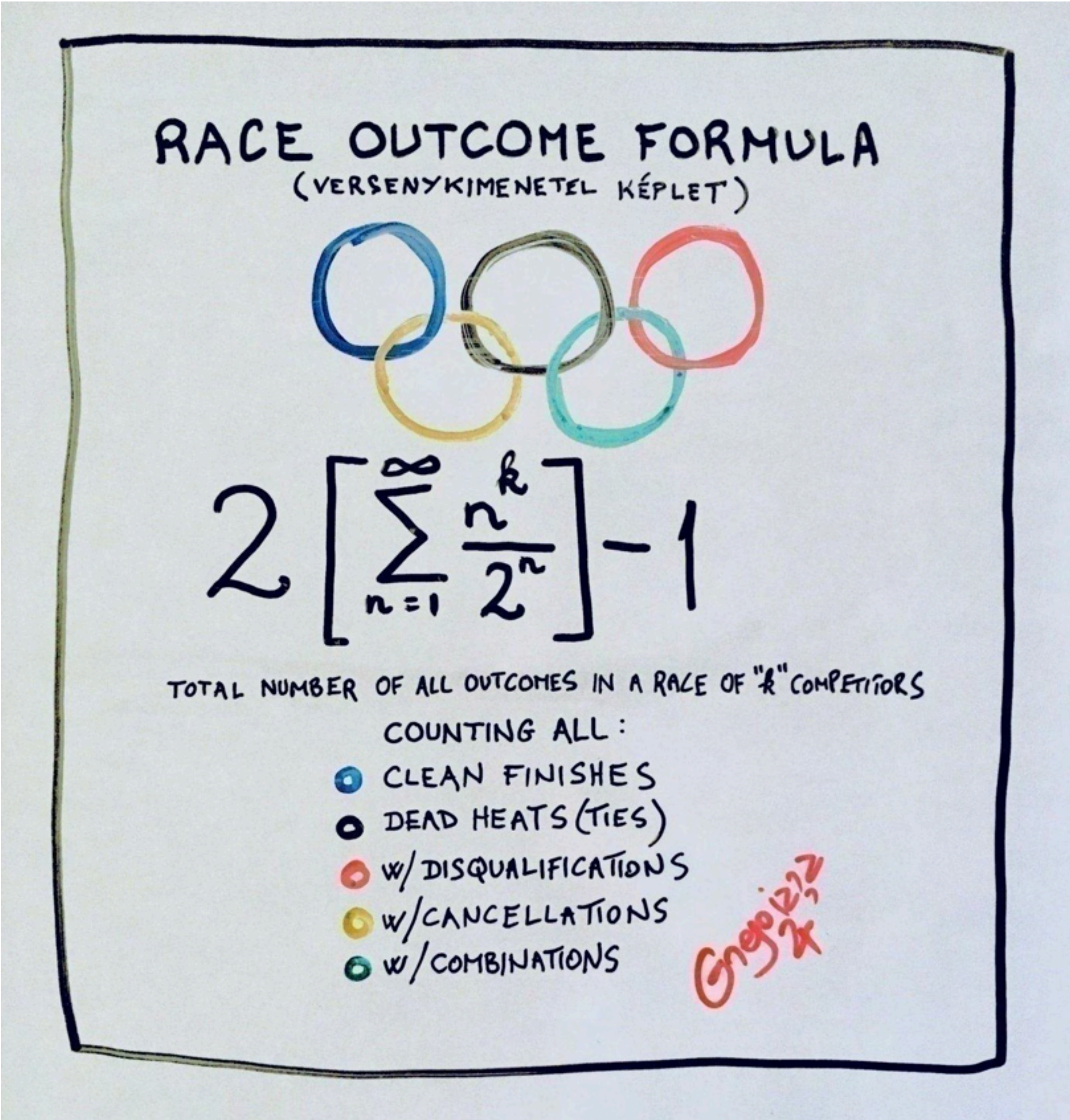

The formula for the number of all predictable outcomes of a race between any given number of registered competitors, where clean finishes, dead heats (ties), disqualifications, cancellations and their combinations are all counted. (11 outcomes for two competitors, 51 for three, 299 for four, etc.). See: The Online Encyclopedia of Integer Sequences (oeis.org/a007047).

At the next retrograde constraint level and in sharp contrast to the two quadcousins, the Quadruplet (0,0,0,0) is at the far end of the relaxation spectrum with its 4 identical magic star diaquad partitions, a totally different realm.

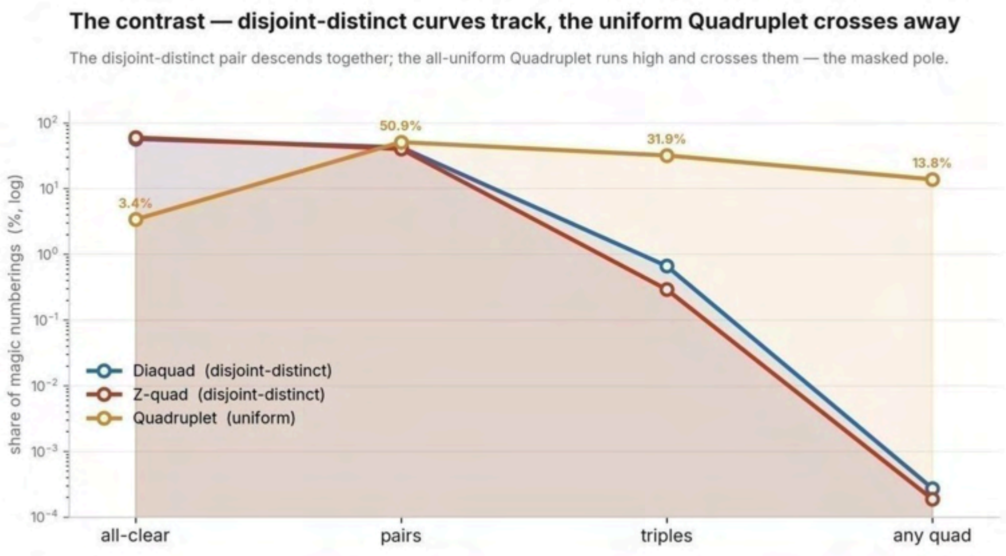

The Quadruplet's masking landscape sharply disagrees with those of the Diaquad & Z-quad censuses, while the latter two seem to closely correlate with the testreliance curve of the various medical specialties.

Photographic study of orthogonal projections of a rhombic dodecahedron in both monochrome and colored versions.

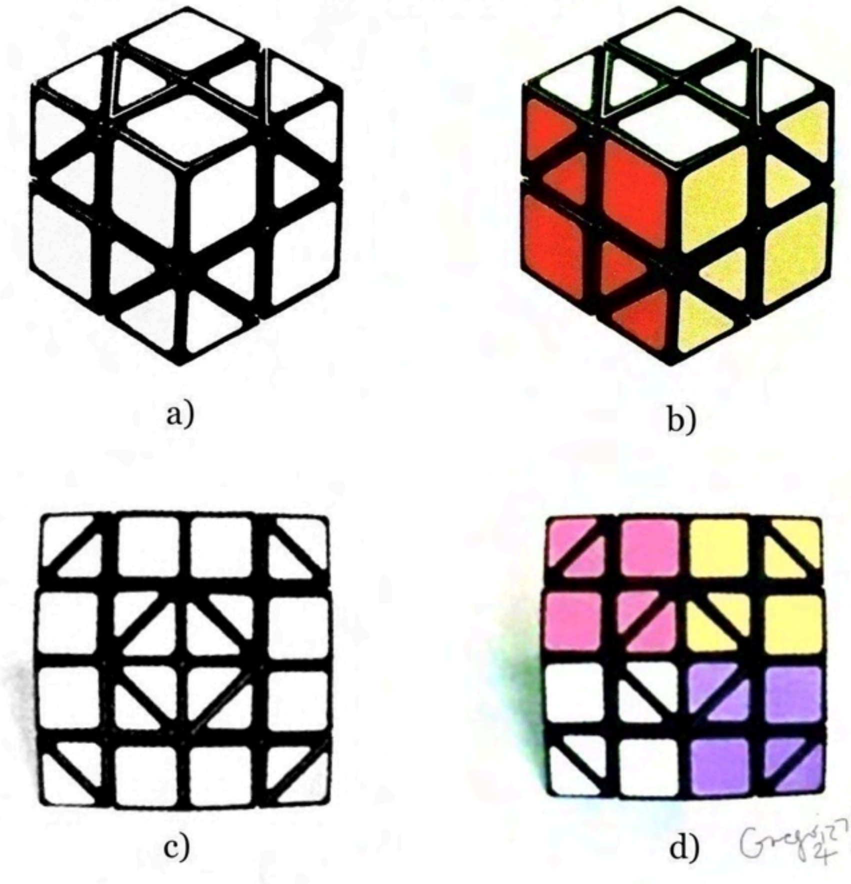

The diagnostic triad across the specialties

From the laboratory disciplines (top) to the clinical ones (bottom): as test-reliance falls, the history — and in hands-on fields the physical exam — takes over.

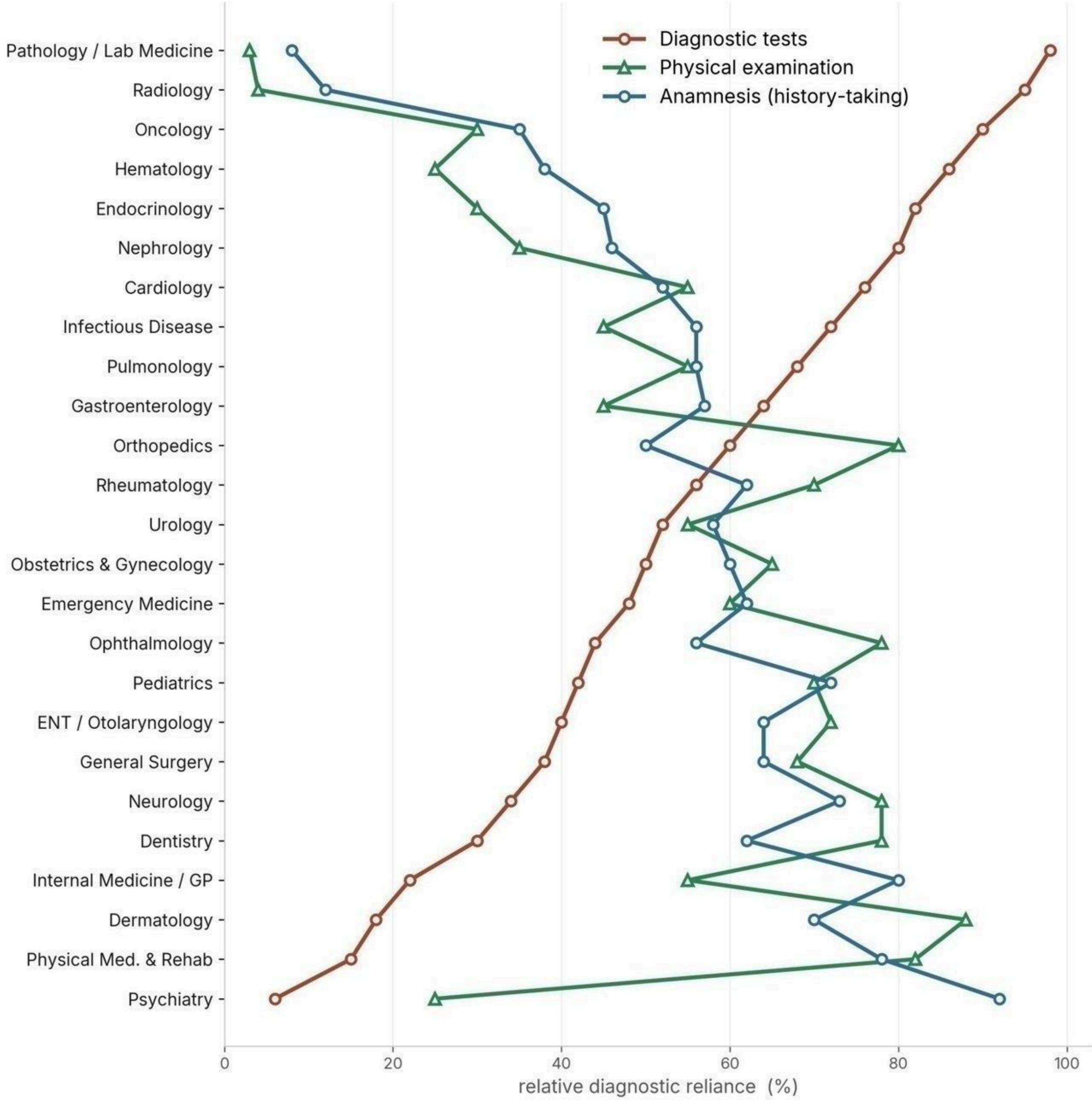

Indicative schema, anchored on the diagnostic-yield literature: history alone gave 82.5% of diagnoses (exam 8.75%, labs 8.75%) [1]; 76% in a US cohort (exam 12%, labs 11%) [2]; 56% [3]. Specialty placement reflects each field's documented diagnostic workflow.

Common blood tests — what they flag and how reliable they are

A companion to the reliability graph. Sensitivity / specificity is shown where a clear figure exists; many panels are monitoring or descriptive, not one-number diagnostic, and are noted so. Refs key to the list.

MARKER	WHAT IT FLAGS	SENS. / SPEC.	REF
CARDIAC & VASCULAR			
hs-Troponin	acute myocardial infarction	99% / 92%	5
NT-proBNP / BNP	heart failure (rule-out)	96% / 47%	13
D-dimer	venous thromboembolism	97% / 41%	6
INFECTION & INFLAMMATION			
C-reactive protein (CRP)	bacterial infection	~80% / 67%	17
Procalcitonin	bacterial sepsis	77% / 79%	12
ESR	inflammation	nonspecific (slow)	—
White cell count (WBC)	infection, inflammation	nonspecific	—
Blood culture	bacteraemia, sepsis	specific; sampling-limited	—
ENDOCRINE & METABOLIC			
HbA1c	diabetes	51% / 96%	18
Fasting plasma glucose	diabetes	49% / 98%	18
TSH	thyroid dysfunction	98% / 92%	15
Lipid panel	cardiovascular risk	risk stratification	—
HAEMATOLOGY			
Haemoglobin (CBC)	anaemia	reference test	—
Ferritin	iron-deficiency anaemia	specific for iron deficiency	—
Platelet count	bleeding / clotting	descriptive	—
TUMOUR MARKERS			
PSA	prostate cancer	86% / 33%	16
CA-125	ovarian cancer	monitoring > screening	—
CEA	colorectal cancer	monitoring, not screening	—
AFP	liver & germ-cell tumours	adjunct + monitoring	—
LIVER & KIDNEY			
ALT / AST	hepatocellular injury	sensitive, nonspecific	—
Creatinine / eGFR	kidney function	functional marker	—
Bilirubin	cholestasis, haemolysis	descriptive	—

Sources keyed [5–18] to the References list. Figures are representative values that shift with population, assay and threshold.

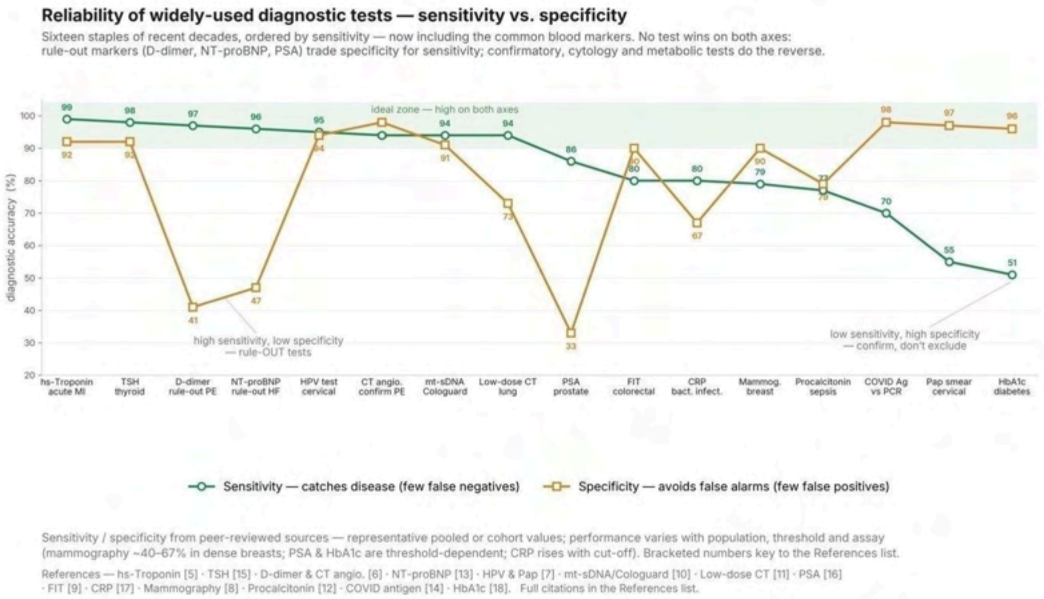

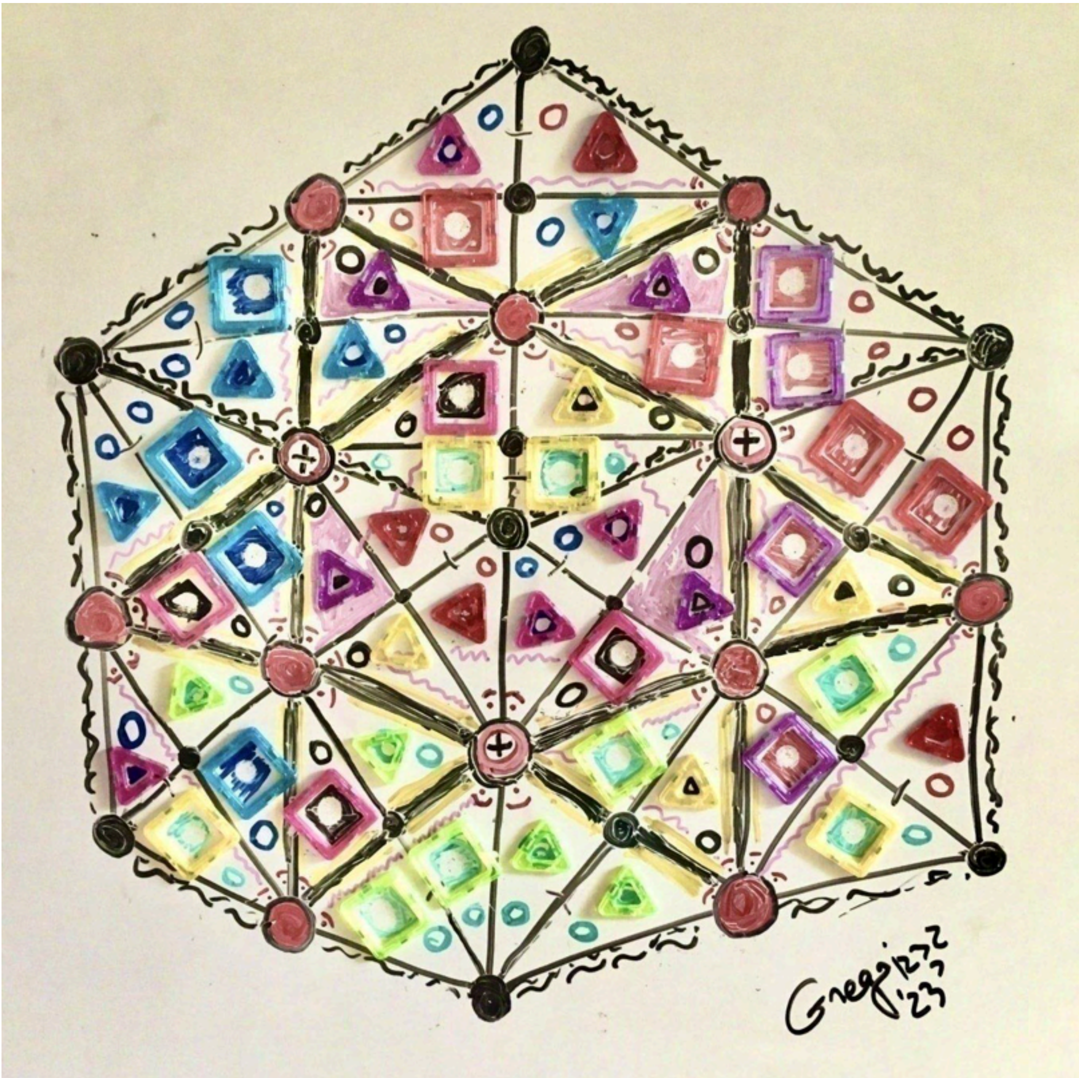

Summetry study with colors and magnetic polygons on whiteboard

RELATED WORKS

The solid in the sciences

Escher's Solid is not only this model's stage; it recurs across the sciences. **Naoki Yoshimoto** found that two of these solids fold together into a cube (each exactly half its volume), an object now in the Museum of Modern Art [S1]. This catalogue grows out of the author's own numbering experiment on the same solid, *„Számozási kísérlet a stellált rombikus dodekaéderen"* was a joint work with **Gergő Kiss** [S5] and **Lajos Szilassi** contributed the GeoGebra construction of the puzzle version of the solid.

Three contemporary uses

Spacetime lattice — Villeponteau

Bryant Villeponteau's Triad Model treats quantum substructures as an active spacetime lattice, and holds that the stellated rhombic dodecahedron has an ideal structure for that lattice. [S2]

Mechanical metamaterials — Vangelatos and colleagues

Microlattices whose unit cell is the first stellation of the rhombic dodecahedron (Escher's Solid) markedly improve the strength and energy absorption of mechanical metamaterials. [S3]

DNA-origami nanoparticles — Pan and colleagues

Scaffolded DNA self-assembles into designed polyhedral nanoparticles; the rhombicdodecahedron family is among the shapes whose structure and dynamics they map at the 5–100 nm scale. [S4]

RELATED WORKS - HECTOQUADS

The squared square model

An alternative realm for the sieve model of medical diagnosis is that of the infinite universe of distinctly squared squares, also reducing to singularity.

The author's painting of the smallest simple perfect squared square (SPSS), featured in the Online Encyclopedia of Integer Sequences published since 1964 by Neil Sloane (oeis.org/a014530). This square dissection, proved to be smallest by Duijvestijn, is also featured as the logo of the Trinity Mathematical Society (TMS) founded in Trinity College, Cambridge in 1919 by G. H. Hardy to "promote the discussion of subjects of mathematical interest".

RELATED WORKS - HECTOQUADS (continued)

Since medical diagnosis-accuracy, test-reliability, as well as demographic, prevalence, incidence and other related data are most frequently expressed as (rounded) percentage-point integers, a new, special class of square dissections with element unit side lengths (s) 1≤s≤100 in various orders of simple perfect squared squares (SPSS), simple imperfect squared squares (SISS), simple perfect squared rectangles (SPSR) and simple imperfect squared rectangles (SISR) was established, which I named Hectoquads.

Interestingly, the smallest singularity among the Hectoquads also belongs to a class of 26 (the number of squares in the square), just like the magic number of the hexagrams and what I label as the transdimensional number, the only positive integer to be sandwiched between two perfect powers, a square and a cube.

The author’s smallest Hectoquad SPSS — 26:274A AJD 1993, both sides 1≤s≤100. — Grego

OEIS®-style contribution

NAME

Side lengths a(n) in the lowest order (26) example of a perfect squared square with 1≤a(n)≤100 and both extreme values present.

DATA

1, 4, 6, 9, 13, 15, 17, 28, 29, 35, 37, 41, 43, 53, 57, 58, 60, 62, 63, 64, 66, 73, 82, 83, 91, 100

COMMENTS

There are conjectured to be no more than seven perfect squares with smallest and largest square-sides sized 1 and 100, of which the present one, 26:274A AJD 1993 (AJD=Prof. dr. ir. A.J.W. “Arie” Duijvestijn) is in the lowest order (26 squares), followed by 29:221A AJP 2011 (AJP=Anderson, Johnson and Pegg), 29:264A AJP 2011, 30:246A (JDS)=Jasper D. Skinner, 31:228A (JBW) 2013, 33:279A JBW 2013 and 35:324A JBW 2016 (JBW=James Williams). In addition, there are an unknown number of dissections with square side lengths within the specified bound without both extreme values (1, 100) or having repeated values; these include simple perfect squared squares (SPSS), simple imperfect squared squares (SISS), simple perfect squared rectangles (SPSR) and simple imperfect squared rectangles (SISR), altogether forming the entire class of Hectoquad squarings (e.g.: 8 out of 8 in order 22, 10/12 in order 23, 4/26 in order 24, 3/160 in order 25, 7/441 in order 26, 3/1152 in order 27, 3/3001 in order 28, 2/7901 in order 29, 9/20566 in order 30, 8/54541 in order 31, 6/144161 in order 32 of simple perfect squared squares).

OEIS®-style contribution (cont.)

REFERENCE

N. J. A. Sloane and Simon Plouffe, The Encyclopedia of Integer Sequences. Academic Press, San Diego, 1995, Fig. M4482.

I. Stewart, Squaring the Square, Scientific Amer., 277, July 1997, pp. 94-96.

LINKS

Stuart E. Anderson, squaring.net/sq/ss/spss/o26/spsso26.pdf, Catalogue of Perfect Squared Squares, Order 26, page 16.

Gergely Földvári, https://www.grego.hu/star - central Escher's solid, Star Face - Grego's Polyhedral Sieve Model for Medical Diagnosis, p. 73

The Joy of Thinking Foundation / *Gondolkodás Öröme Alapítvány* - Hungary EU, Nationwide open online mathematical problem solving project "minden·ki·jön Day 19" paragraph 2, 7 May 2025 (https://www.mindenkijon.hu/p/mindenkijon-19-nap)

Trinity College Mathematical Society, https://tms.soc.srcf.net/about-the-tms/the-squared-square/ — The Squared Square.

Wikipedia https://en.wikipedia.org/wiki/Squaring_the_square — Squaring the Square.

EXAMPLE

Bouwkamp Code: 26 274 274 (91,100,83) (17,66) (82,9) (73,53) (4,62) (57) (58,60,37) (29,64,1) (63) (43,15) (13,41,6) (35) (28)

CROSSREFS A014530

KEYWORD nonn, fini, full

AUTHOR Gergely Földvári

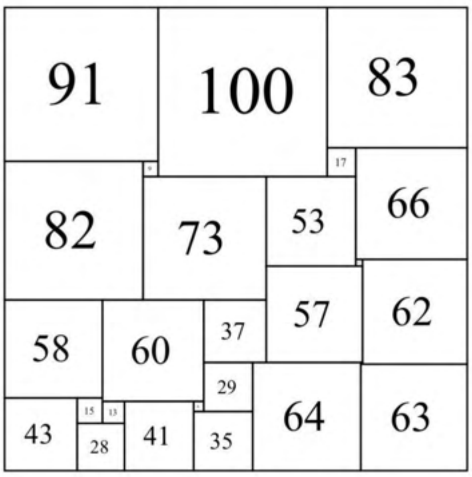

26 : 274A AJD 1993

Stuart E. Anderson's On-line Catalogue, Order 26 SPSS, p. 16

RELATED WORKS - HECTOQUADS (continued)

PIXEL PARADOX

An interesting visual representation aspect is the challenge in displaying such square dissections featuring a unit-sized square, pinpointed here as an odd-one-out puzzle called the Pixel Paradox:

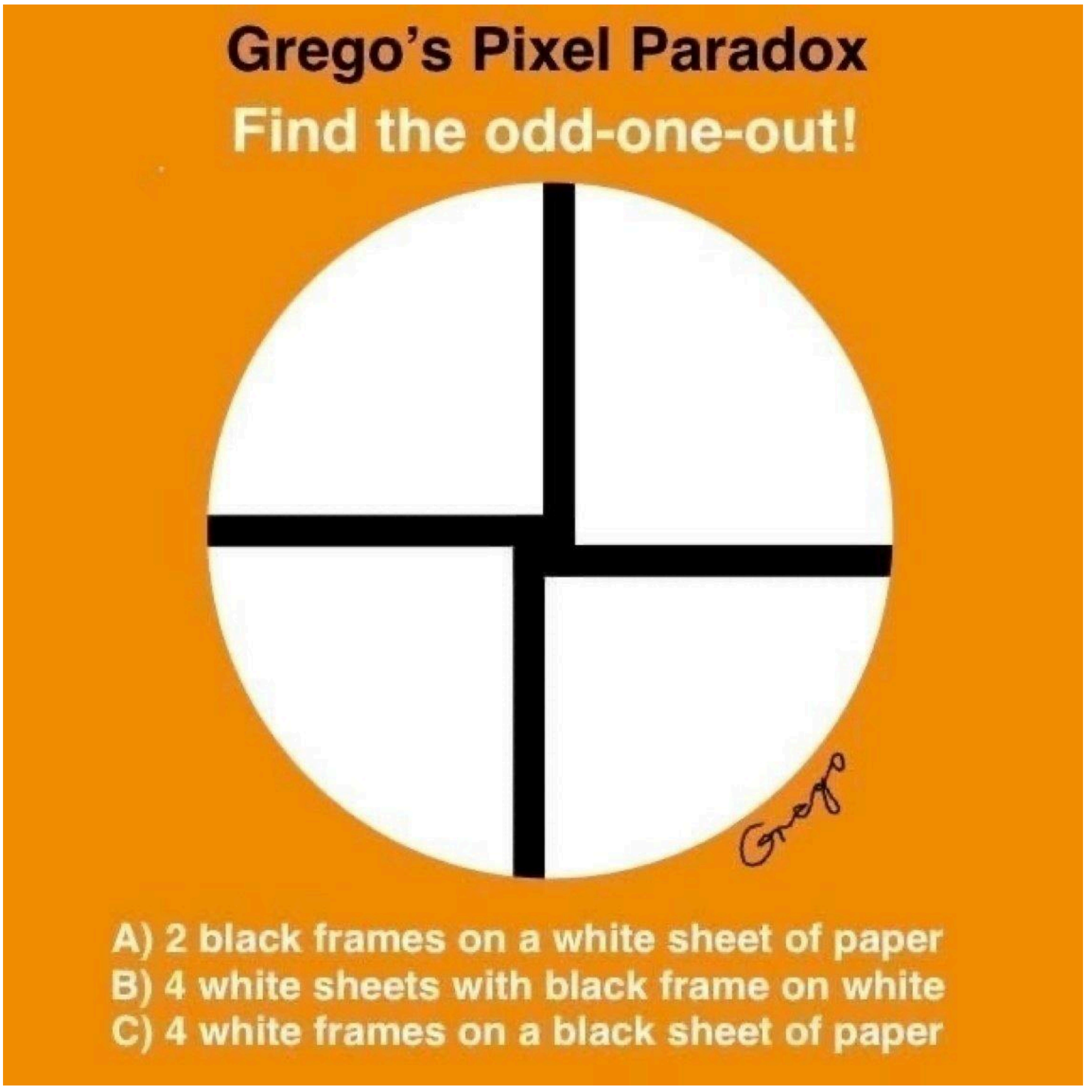

Grego's Pixel Paradox — find the odd one out — Grego

RELATED WORKS - GEMATRIA

SACRED SUMMETRY OF MAGIC SUM 26

The model's magic constant 26 is the highly revered numerical sum value (gematria) of the sacred biblical Tetragrammaton composed of the Hebrew letters yod (10) + hey (5) + vav (6) + hey (5), carrying far-reaching cabalistic significance. The partition (10,5,6,5) is one of 26 that the Escher solid's 12 pyramids can read with one repeated number from {1-12} on the 12 diaquads of the four disjoint-distinct star face hexagrams.

SUMMETRY

The cube-derived Escher solid's 13 rotational symmetry axes cross its surface 26 times and together with their 13 perpendicular symmetry planes, yield 26 as the full symmetry tally: 13 roto-reflect symmetry axes + 9 mirror-reflect and 4 roto-reflect symmetry planes.

FORMULA

$a(n) = (((n-1) \bmod 9)+1) \cdot 10^{\lfloor (n-1)/9 \rfloor}$, $1 \le n \le 22$

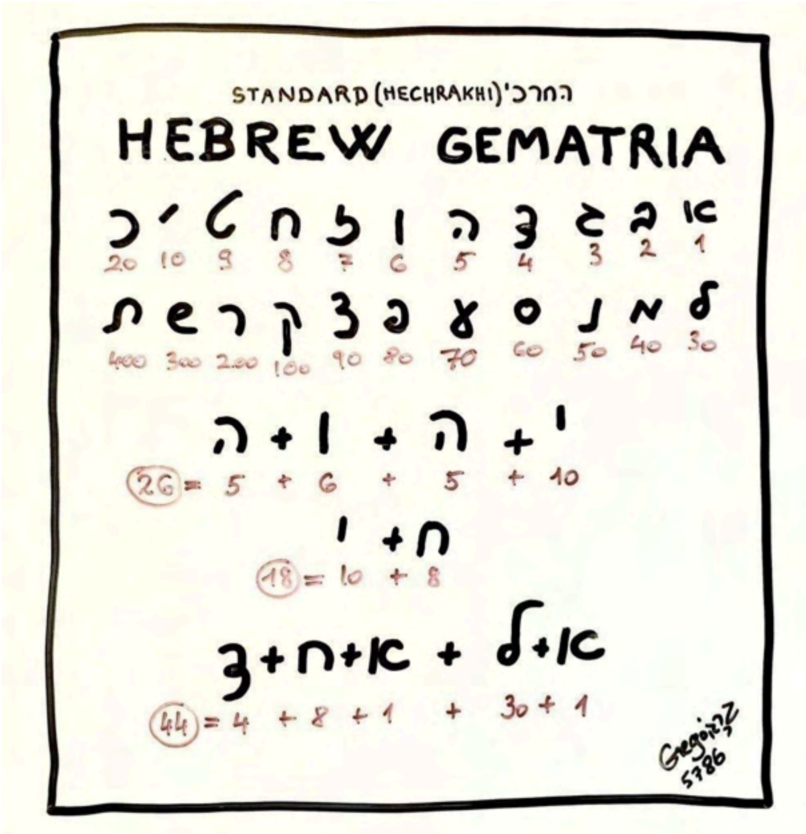

Standard (Hechrakhi) Hebrew Gematria — source: oeis.org/A051596

RELATED WORKS — TABAKGASSE POLYHEDRON

BUDAPEST DOHÁNY UTCA (TABAKGASSE) SYNAGOGUE LANTERN

With a 3D model by Vera Viana, source: tinyurl.com/tabakgasse

EULER CHARACTERISTICS

i) after square-hexagonal truncation of cube

Faces 14 · Edges 28 · Vertices 16

16 - 28 + 14 = 2

ii) after augmentation of polyhedron with triangle and hexagon based pyramids

Faces 50 · Edges 76 · Vertices 28

28 - 76 + 50 = 2

iii) after complete augmentation with (triangle, square and hexagon based) pyramids

Faces 56 · Edges 84 · Vertices 30

30 - 84 + 56 = 2

RELATED WORKS — TABAKGASSE POLYHEDRON (continued)

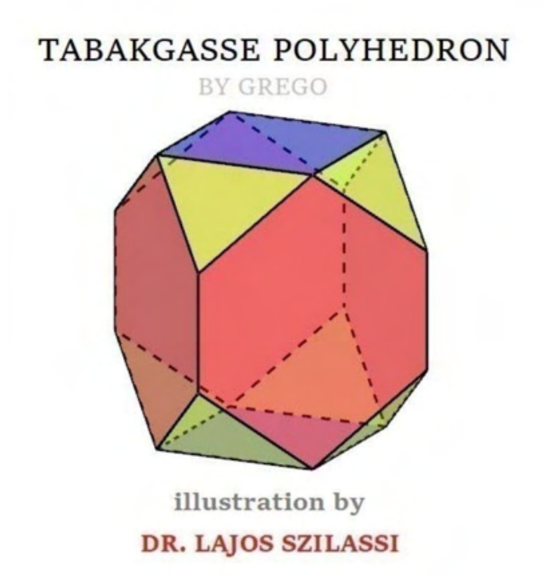

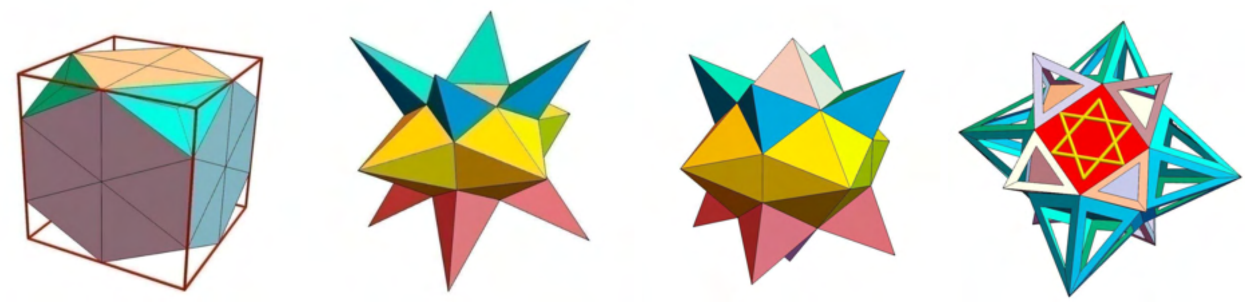

Illustrations by Lajos Szilassi (top), Sándor Kabai (1946-2024), Synagogue photo by Grego

source: tinyurl.com/tabakgasse

RELATED WORKS - MUSIC AND THE SOLAR SYSTEM

THE CONNECTION REVEALED

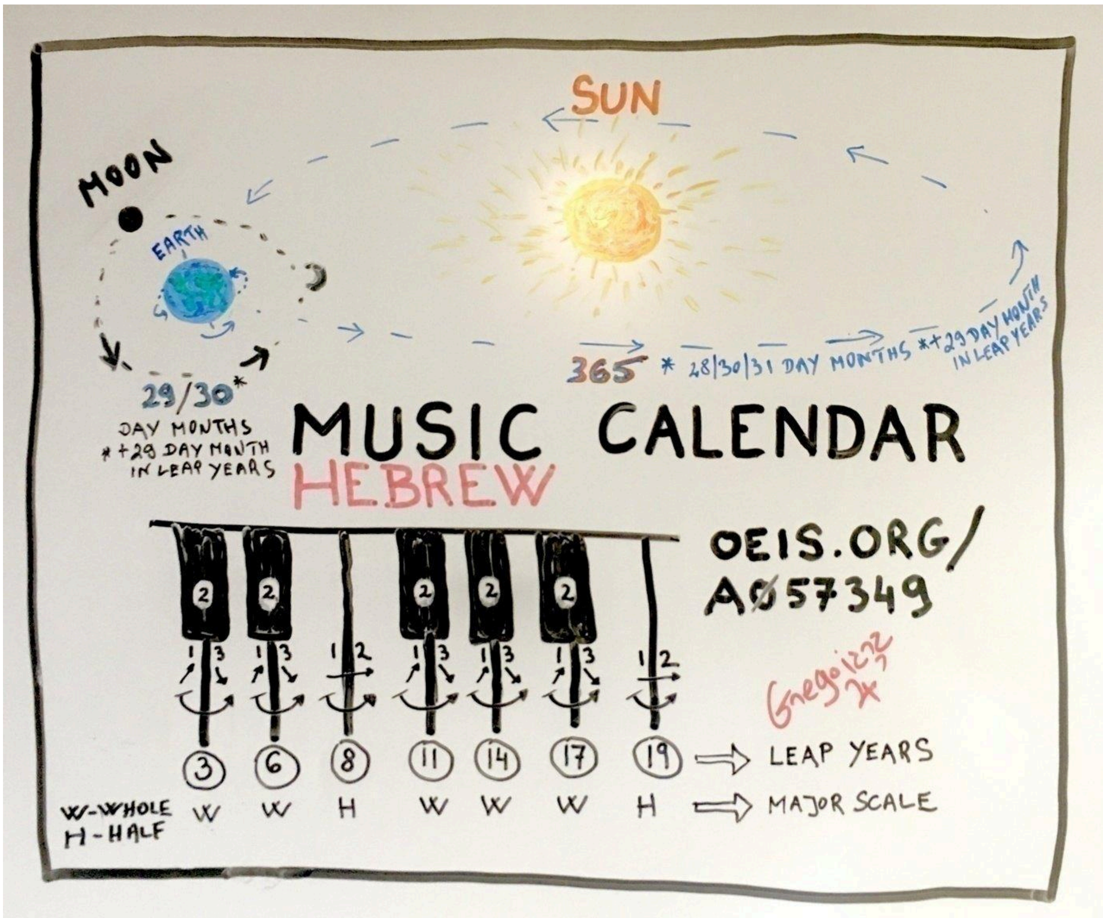

Lunisolar calendar's leap-year cycle as music scale, source: oeis.org/a057349

In equal musical temperament, when an octave is divided into twelve equal half steps (a half step involves two notes and a whole step involves three notes, giving a total of 13 notes including the octave), whole (w) and half (h) step intervals of the major scale follow a pattern of 2w-1h-3w-1h. Assigning the integer 2 (notes) to the half-step and 3 (notes) to the whole-step intervals will result in the same sequence as the placement of leap years in the Biblical (Hebrew/Jewish) lunisolar calendar's 19-year cycle when applied to the major scale of music (ionian among the 7 modal scales and the principal of its relative minor). Source: oeis.org/a057349

Nota bene: the current year 2026 = 5786 when 5+7+8+6 = **26** is a rare occurrence of the magic constant itself, determining the polyhedral summetry sieve model, as well.

RELATED WORKS

SPIN-OFFS

Transdimension & Summetry on the Platonic Solids

The summetry principle (a balance that arises from the symmetry itself) carried beyond the star onto the tetrahedron (face corners 1-12 → edge quadruples 26), octahedron (edges 1-12 → vertices 26), cube (edges 1-12 → faces 26, see GooglyCube), dodecahedron (trapezoid/triangle partitioned faces or main slope trapezoid and coplanar hip-end triangles of hip-roofed nested cube 1-12 → ridges 26), icosahedron (vertices 1-12 → x,y,z edges 26).

Coefficial Divisibility

Multimorphism, transdimension and singular incidence approached through the folklore result that 26 is the only integer wedged between two perfect powers, the same twenty-six that is this model's magic sum. Does it make sense to divide zero? Can 2 pebbles be thrown by four boys? [S6]

VIO Formula and GooglyCube

Simple geometric formula: a cube's edge times its body-diagonal, over its face-diagonal, equals the diameter of its largest inscribed circle; and a tactile cube game object grown from the same summetry as the present model itself, in fact the cubic puzzle game version of the work at hand, designed by the author and expected to go on sale worldwide in 2026 (googlycube.com).

Metatron Numbers and New Integer Sequences

Contributions to the On-Line Encyclopedia of Integer Sequences, e.g. oeis.org/A387889 and A387890 (first differences of consecutive odd / even perfect powers). The new Metatron Number geometric constants fully derived at tinyurl.com/GregosMetatronNumbers. [S7]

Survival Formula, Collective Survival Threshold (CST)

A chart of the survival threshold of the hundred-prisoners loop strategy (the least number of choices that keeps the chance of success above one-half), whose first singletons fall on the Fibonacci primes two, three and five. (On-Line Encyclopedia of Integer Sequences, A389262.)

Grego's Limbo Match

A memory-and-strategy game for all generations based on that same Critical Survival Threshold (CST), the point at which the loop strategy success tips past one-half (oeis.org/A389262), play free and up your score in the GLM100 Ranking to become a World Champion, at grego.hu/limbo.

RELATED WORKS SPIN-OFFS ILLUSTRATED

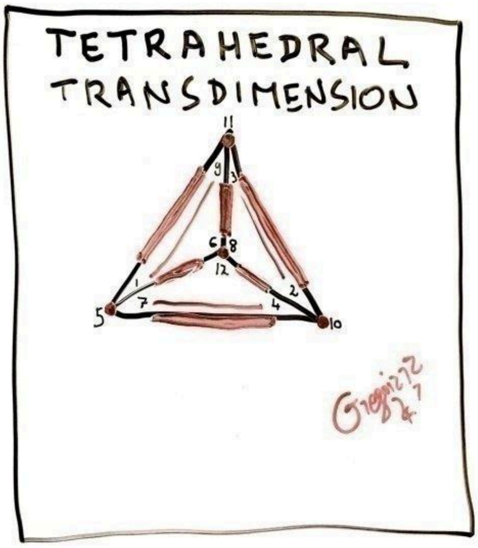

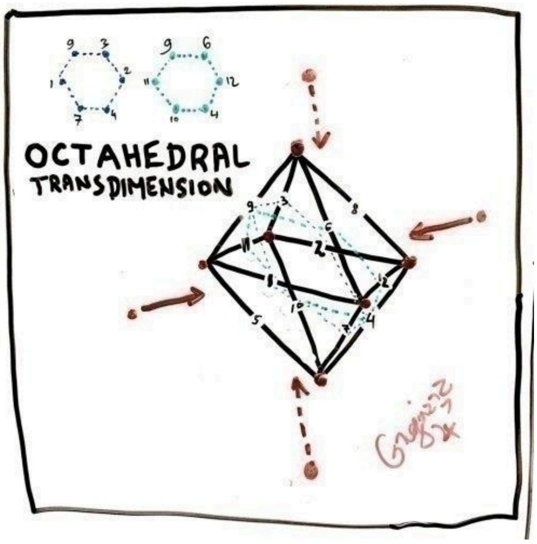

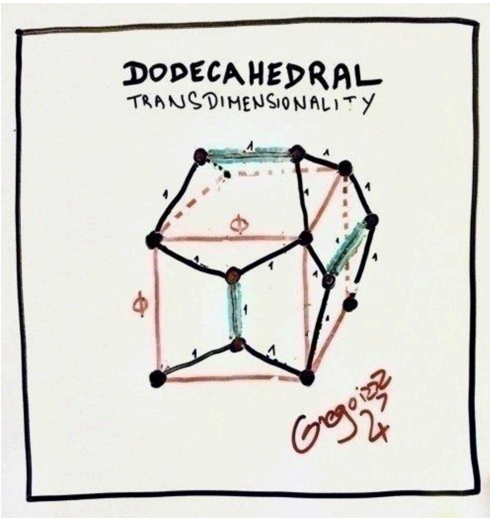

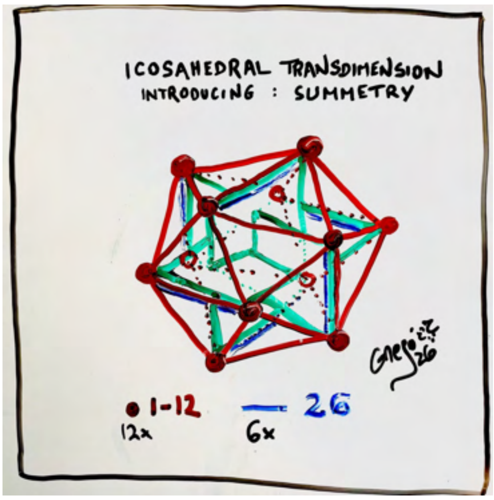

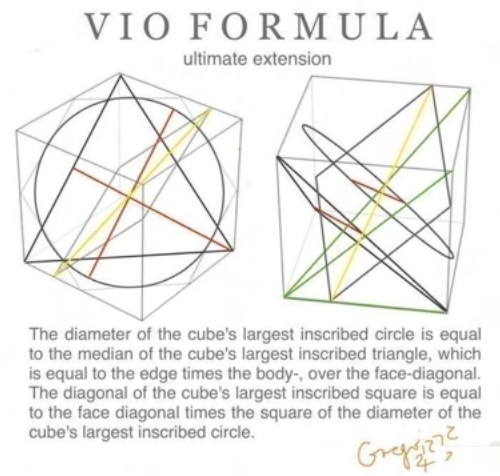

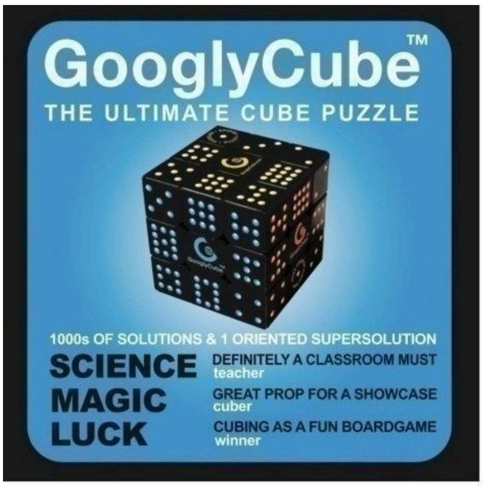

Illustrations of the author's spin-offs

Transdimension & Summetry on all five Platonic solids (tetrahedron, octahedron, dodecahedron, icosahedron, cube - GooglyCube.com), novel VIO Formula: "cube edge times body-, over face-diagonal equals diameter of largest inscribed circle"

RELATED WORKS SPIN-OFFS ILLUSTRATED (continued)

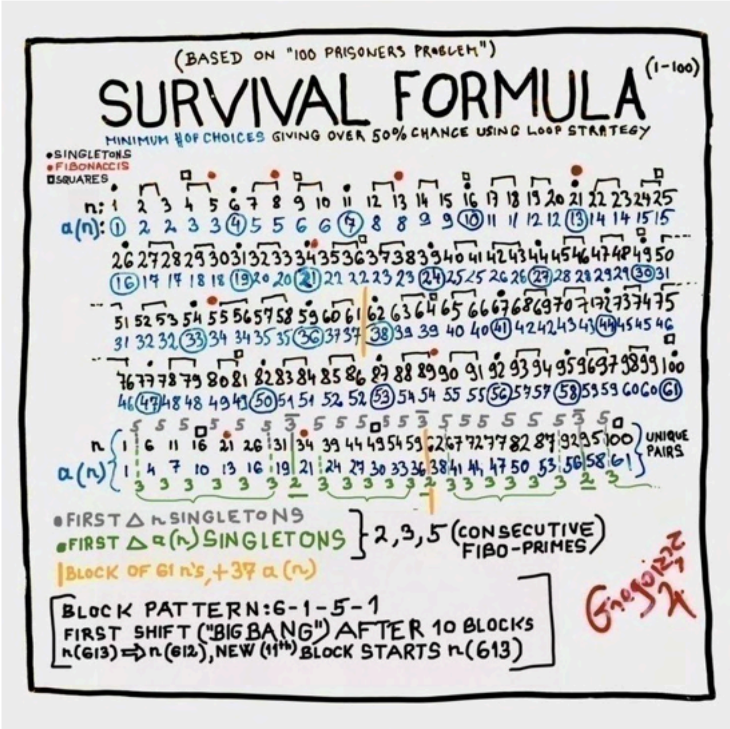

Collective Survival Threshold (CST) >50% based on loop-strategy, oeis.org/A389262,

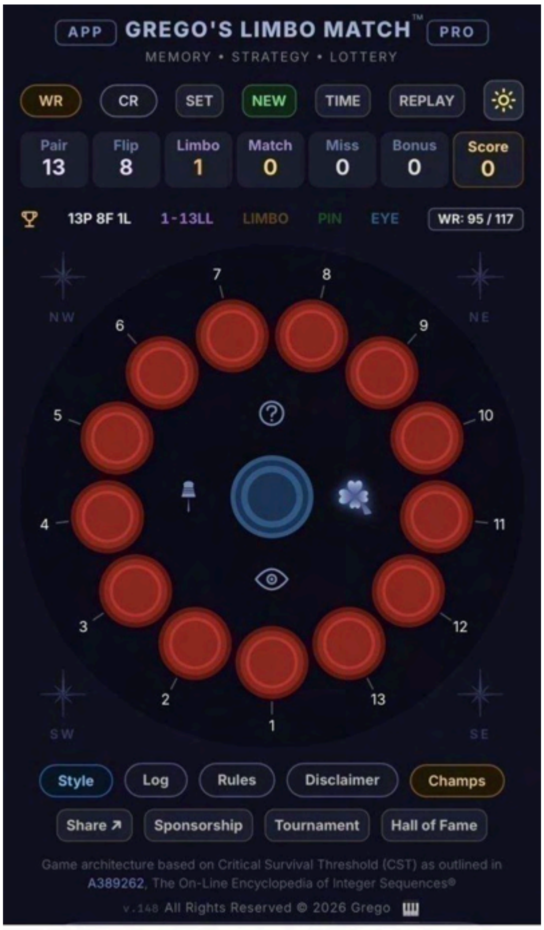

Grego's Limbo Match, CST as a strategic memory game at grego.hu/limbo

RELATED WORKS – METATRON NUMBERS

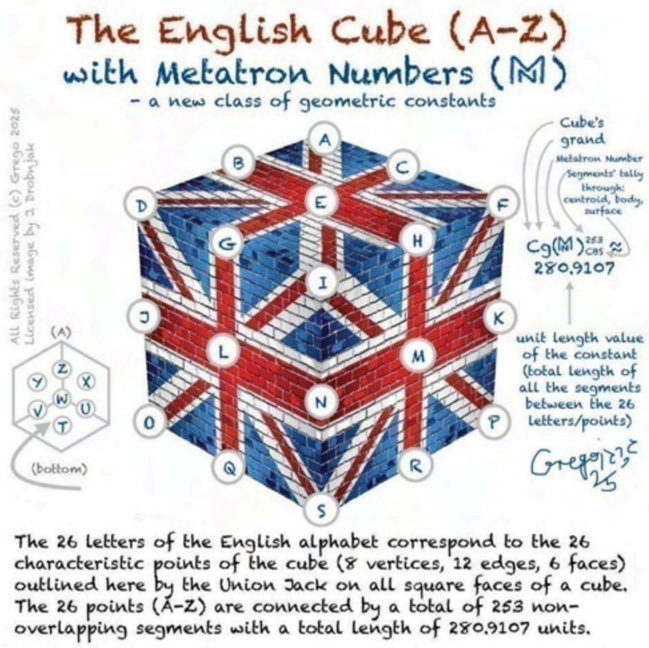

The English Cube (A–Z): the twenty-six letters at the cube's twenty-six characteristic points.

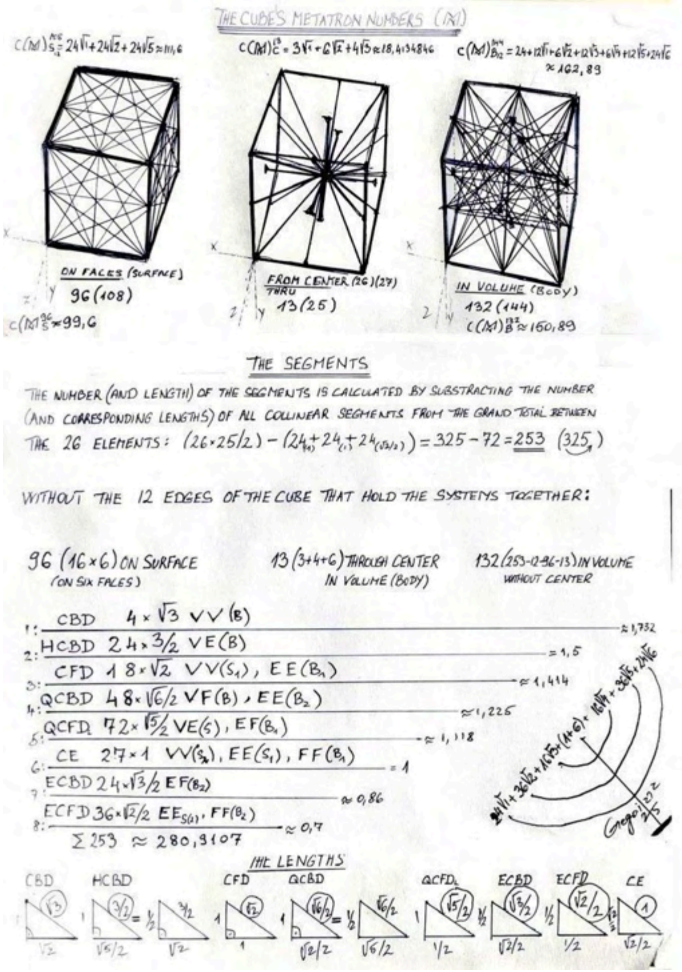

The cube's Metatron Numbers — segments on faces, through centre and body — worked by hand

CONCLUSION

AN OPEN PROPOSAL FOR FUTURE RESEARCH

Escher solid's 48 faces presented a factorial numbering that is over the Solar System's atom count now down to that of a human embryo, the three sieves of the model leave a structure: a magic star whose twelve pyramids each carry one reading, bounded above and below, with masking that is graded, always possible, and, save one exception, escapable. This closing chapter puts that structure forward (as a proposal, not a finding) to become a candidate vocabulary for one of medicine's oldest problems: hearing hoofbeats and deciding whether to look for a zebra. Let each of the twelve pyramids stand for a diagnostic reading. A mask (two or more pyramids sharing the same four values) is a condition wearing a common look-alike's face. The landscape then says three things at once. A clean, fully distinct reading exists for every combination but one: the zebra can almost always be isolated. Masking is always possible: the zebra can always be made to hide. And the heaviest mask cannot appear quietly (at its deepest the masking leaves no clear reading at all), so the gravest case forces itself, eventually, into the open. The zebra can be found, after all.

The model also keeps the human factors in view: the caregiver's finite attention under stress, the patient's age and the slow, vague onset of the rarest disorders. Against a field of thousands of rare diseases, a sieve that shows a distinct reading nearly always exists (and bounds how badly the truth can hide) is offered here as a direction worth formal study, not as a clinical instrument.

A word of extra special and heartfelt thanks to distinguished mathematicians and professors, entrepreneurs and friends, Vera Viana, Stuart E. Anderson, Lajos Szilassi, Dániel Erdély, Gergő Kiss, Dirk Huylebrouck, Neil Sloane, Izidor Hafner, William Heyman, György Birkás, Péter Érdi, Tamás Kósa, Domonkos Tikk, Bruno Fuchs, Gábor Verebes, Dávid Friedman and Zsuzsanna Friedman, Regina Hellwig-Schmid, Andrea Szegő, Judit Dutka, Viktor Orosz, András and Antal Csóka, Tamás Vészi, László Ladislav Pálmai, Gábor Kádár and Zoltán Vidák, for their continued support during my research, and remembering Sándor Kabai, some of whose last works are presented here for the first time.

CONCLUSION (continued)

READING THE ZEBRA - HOW THE PAST PRESENTS THE FUTURE

Addison's disease is rare, about one in hundreds of thousands, or less. The adrenal cortex fails, cortisol and aldosterone fall, and the early signs are vague: fatigue, nausea, low mood, low blood pressure, a craving for salt. Thomas Addison described it in 1855; John F. Kennedy lived with it. Because the picture is so ordinary, diagnosis is often delayed. Picture a sixty-year-old read, for years, as depression, then as irritable bowel, then simply as ageing, with antidepressants tried, steroid tablets prescribed and taken, the true cause missed, the hormones are not produced anymore as the cortex falls asleep due to the tablets.

In the model's terms, these are masked pairs: a rare reading hidden behind common look-alikes. Yet the landscape promises a distinct reading exists, and here it does: on the skin. Darkening where the skin creases (the potentially lifethreatening tan) and, tellingly, patches of vitiligo: an autoimmune signature that breaks the mask and names the zebra. For the lucky ones, *ex juvantibus* therapy, a swift recovery and a short test (ACTH stimulation) confirms it; replacing the missing hormones treats it. And the singularity has its clinical echo: the maximal collapse, an Addisonian crisis cannot stay hidden; it announces itself. The danger is real but bounded and its worst form cannot appear quietly.

Woodward's zebra words, like those of Occam's razor withstand time: no physician, not the ambitious young medic, neither the highly qualified, nor the much sought after doctors whose patients queue up on waitlists can escape it, while none can be expected to disregard the hoofbeats and hyperfocus on untying what often seems like a Gordian knot, especially hard when anamnestic data are obscure or overwhelming. But cutting the knot is exactly what is being proposed here, through a model that can, and hopefully will be implemented using human programming ingenuity, hand in hand with the computing prowess of artificial intelligence.

Ars longa, vita brevis. Rest assured, true for millennia and will stay true for more, even if nano-technology some day soon bio-powers data-collection, storage and processing, for two simple reasons: our bodies ail and electricity can be scarce, or cut. No A.I. or robot can substitute a devoted human physician's fingers on your wrist, the touch of the glands under your chin, a good look in the mouth or a gentle tap of percussion on the back. But as long as there is development and there is also electricity, we can all see how things do improve, how life expectancy extends.

Special thanks to our family's now fourth generation friend and physician, chief surgeon Dr. Gábor Friedman (Semmelweis University, Budapest, Hungary) for long-standing support and care, and also to general practitioner Dr. János Ávéd (Praxis of the Year Awardee, 2017, Mindszent, Hungary) for providing invaluable diagnostics information for my research.

Ars longa, vita brevis - Semmelweis University Clinic, Budapest, photo by Grego

ANAMORPHOSIS

The Anamorphosis of Numbers

How transdimensionality surfaces in illustration

Carefully nuanced oblique anamorphosis was used in placing the integers on the orthographically projected polyhedral model in the 3D animated illustrations on grego.hu/star: each number is pre-skewed within its own slanted face so that, viewed head-on, it projects to the viewer as an upright, undistorted figure, compensating for the foreshortening and slant that would otherwise arise from the oblique angles of the 48 congruent isosceles triangle faces, had the numbers simply been drawn upright on each face as on a flat label.

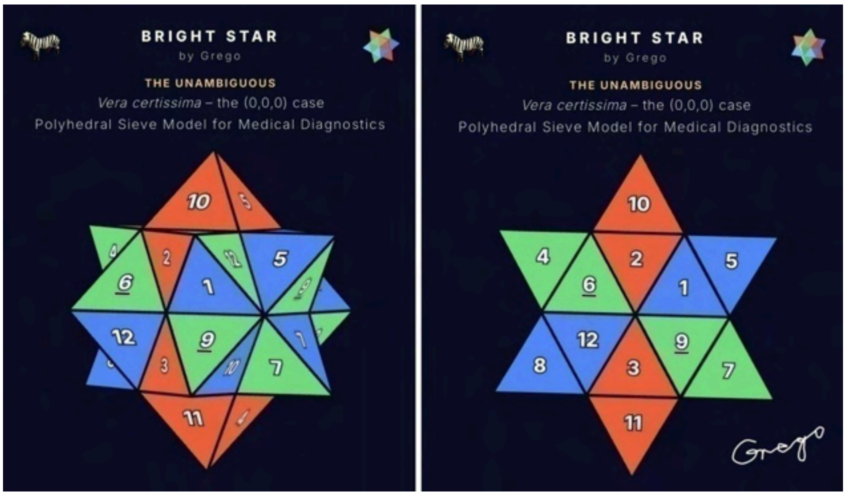

two different orthographic views of a magic star on the interactive BRIGHT STAR ‘Vera certissima’, the case of (0,0,0), i.e. no identical (pair, triple, quadruple) readings among the 12 pyramids (pyraquads), all different partitions summing to the magic number 26 → a certain diagnosis by the model; left as quasi 3D, right 2D

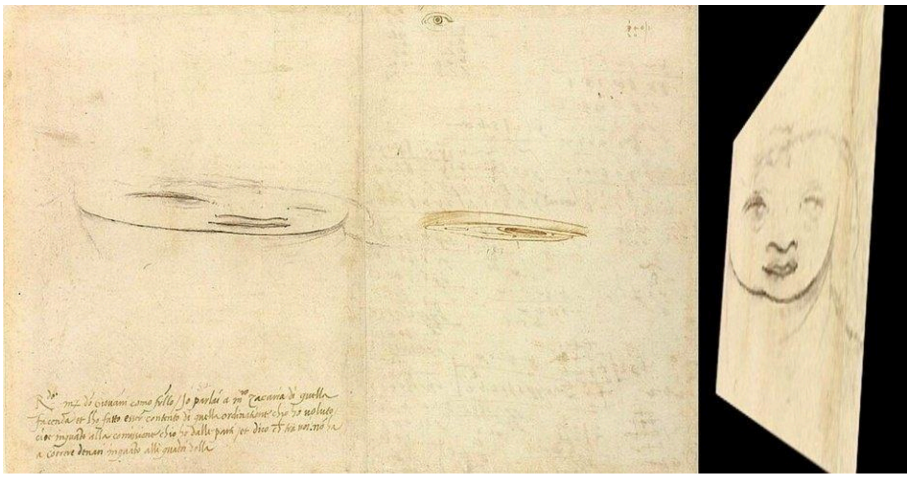

Leonardo da Vinci’s anamorphic child face sketch “*Occhio Bambino”*, *Codex Atlanticus* (1515); https://codex-atlanticus.ambrosiana.it

Compare: Hans Holbein the Younger “The Ambassadors” (1533), see page 96

THE ALPHA-OMEGA AXIS – SYNAPSIS AND SYNOPSIS

Upon acquainting my endeavors per the present study, a learned friend casually remarked about my entanglement with the two, close-sounding notions. It wasn't until the recent relief brought about by the satisfying results outlined above in the paper that I could finally reconcile.

Synapsis ***σύναψις*** *σύν* "together" + *ἅπτειν* "to fasten, to touch"

A joining by contact. In meiosis it pairs homologous chromosomes so they can cross over and trade material; in the brain it is the synapse, where a cell reaches across a gap to touch and signal another. **Togetherness made by touching**.

Synopsis ***σύνοψις*** *σύν* "together" + *ὄψις* "sight, view"

A seeing together: the whole held in one glance, the survey that shows at once what one would otherwise walk through piece by piece. **Togetherness made by seeing**.

Both are acts of "with," through different organs. Synapsis joins by touch: local, generative, a meeting where something passes between two things. Synopsis joins by sight: global, the whole field grasped from above. One is a junction, the other an overview.

synApsis → synΩpsis

one vowel turns the junction into the overview; alpha becomes omega

And not only in play: a synopsis is what a dense web of synapses finally yields, because comprehension is connection seen whole. Understanding begins as one synapse and matures into a synopsis, the whole territory surveyable at a glance. This is the axis from alpha to omega in a life's work. It can begin in an instant: a serendipitous touch, or a form glimpsed once, is a single synapse. Between that chance encounter and the finished view lies the gap, and the gap is measured in years. To close it is the patient work of turning one fastening into one seeing. There is also a rarer road, one perhaps never travelled, on which you do not close the gap but walk the axis itself, holding the live wire of the first touch all the way to the overview, so that the synopsis never forgets it was once a spark. Alpha holds hands with omega for the full length of the road.

REFERENCES

Frontier-diagnostics

[R1]

Photon-Counting CT in 2026: From Innovation to Clinical Impact. ISCT, 2026. isct.org/computedtomography-blog/2026/3/23/photon-counting-ct-in-2026 ; PCCT vs energy-integrating CT in lung cancer, Radiology 2026, pubs.rsna.org/doi/10.1148/radiol.251663 ; FDA clears portable photon-counting CT, Imaging Technology News 2026, itnonline.com/content/fda-approves-portable-photon-counting-ct-scanner

[R2]

uEXPLORER total-body PET/CT, United Imaging, eu.united-imaging.com/en/productservice/products/mi/uexplorer ; EXPLORER total-body PET, UC Davis, explorer.ucdavis.edu

[R3]

The use of hyperpolarised 13C-MRI in clinical body imaging to probe cancer metabolism. PMC8007617. ncbi.nlm.nih.gov/pmc/articles/PMC8007617

[R4]

Transforming cancer screening: the potential of multi-cancer early detection (MCED) technologies. PMC11785667. ncbi.nlm.nih.gov/pmc/articles/PMC11785667

[R5]

CRISPR-based diagnostics for infectious diseases. Front. Cell. Infect. Microbiol. 2026, doi 10.3389/fcimb.2026.1769226 ; Point-of-care next-generation CRISPR rapid diagnosis. Clin. Exp. Med. 2025, doi 10.1007/s10238-024-01540-8 ; CRISPR-driven diagnostics: clinical efficacy and translational challenges. PMC12464570

[R6]

Emerging electronic-nose design for breath-based cancer diagnostics. ACS Sensors 2026, doi 10.1021/acssensors.6c00796 ; eNose vs GC-MS in COPD. BMC Pulm. Med. 2025, doi 10.1186/s12890-025-04040-x

[R7]

The current landscape of plasma proteomics. bioRxiv 2025, doi 10.1101/2025.02.14.638375 ; SomaScan platform validation, SomaLogic 2026, somalogic.com/blog

REFERENCES (continued)

[R8]

Wireless, regenerable multimodal wearable sweat sensor. Nat. Biomed. Eng. 2026, doi 10.1038/s41551-026-01670-2 ; Stressomic wearable stress-hormone biosensor. Sci. Adv. 2025, doi 10.1126/sciadv.adx6491

[R9]

Progress in clinical magnetocardiography: the contactless breakthrough. Sensors 2026, doi 10.3390/s26041369 ; PMC12943995

[R10]

Photoacoustic microscopy for biological visualization and clinical translation. Adv. Sci. 2026, doi 10.1002/advs.202521173 ; A review of clinical photoacoustic imaging. Photoacoustics 2019, sciencedirect.com/science/article/pii/S2213597919300679

[R11]

Hybrid photoacoustic and fast super-resolution ultrasound imaging. Nat. Commun. 2023, doi 10.1038/s41467-023-37680-w ; In-human ultrasound localization microscopy on a clinical scanner, arXiv:2009.13477

[R12]

AI-enhanced retinal imaging as a biomarker for systemic diseases. Theranostics 2025, doi 10.7150/thno.100786 ; Insights into systemic disease through retinal-imaging oculomics (term coined). TVST 2020, doi 10.1167/tvst.9.2.6

[R13]

Towards a general-purpose foundation model for computational pathology. Nat. Med. 2024 ; Generalist radiology foundation model. Nat. Commun. 2025, doi 10.1038/s41467-025-62385-7 ; Generative AI and foundation models in radiology. Radiology 2025, doi 10.1148/radiol.242961

REFERENCES (continued)

Diagnostic-yield & test-reliability

[1]

Hampton JR, Harrison MJ, Mitchell JR, Prichard JS, Seymour C. Relative contributions of history-taking, physical examination, and laboratory investigation to diagnosis and management of medical outpatients. Br Med J. 1975;2(5969):486–489. doi:10.1136/bmj.2.5969.486 — history alone gave 82.5% of diagnoses (exam 8.75%, labs 8.75%).

[2]

Peterson MC, Holbrook JH, Von Hales D, Smith NL, Staker LV. Contributions of the history, physical examination, and laboratory investigation in making medical diagnoses. West J Med. 1992;156(2):163–165. — history 76%, exam 12%, labs 11%.

[3]

Sandler G. The importance of the history in the medical clinic and the cost of unnecessary tests. Am Heart J. 1980;100(6 Pt 1):928–931. doi:10.1016/0002-8703(80)90076-9 — history decisive in 56%.

[4]

Roshan M, Rao AP. A study on relative contributions of the history, physical examination and investigations in making medical diagnosis. J Assoc Physicians India. 2000;48(8):771–775. — history 78.6% (corroborating anchor).

[5]

hs-Troponin (acute MI) — 99% / 92%. Characterization of Myocardial Injury With High-Sensitivity Troponin. PMC10751476, 2023 — sensitivity 99%, specificity 91–92% at the sex-specific 99th-percentile threshold.

[6]

D-dimer & CT-pulmonary angiography (PE) — 97% / 41% and 94% / 98%. Systematic review and meta-analysis of test accuracy for the diagnosis of suspected pulmonary embolism. Blood Advances (Am. Soc. Hematology). 2020;4(18):4296–4311.

[7]

HPV test & Pap smear (cervical) — 95% / 94% and 55% / 97%. Pap Smear vs. HPV Screening Tests for Cervical Cancer. Am Fam Physician. 2008;77(12):1740, summarizing the Canadian Cervical Cancer Screening Trial (Mayrand MH et al. N Engl J Med. 2007;357:1579–1588. doi:10.1056/NEJMoa071430).

[8]

Mammography (breast) — ~79% / ~90%. National Cancer Institute. Breast Cancer Screening (PDQ®) — Health Professional Version. cancer.gov — overall sensitivity ≈79%, lower (≈40–67%) in dense breasts.

[9]

FIT (colorectal) — ~80% / ~90%. Colorectal-screening literature; representative pooled values (e.g. FIT comparator arm of [10], sensitivity 73.8%; reviews reporting ≈80–88% / ≈90%).

[10]

mt-sDNA / Cologuard (colorectal) — 94% / 91%. Imperiale TF, Porter K, Zella J, et al. Next-Generation Multitarget Stool DNA Test for Colorectal Cancer Screening. N Engl J Med. 2024;390(11):984–993. doi:10.1056/NEJMoa2310336 (BLUE-C) — CRC sensitivity 93.9%, specificity for advanced neoplasia 90.6%.

REFERENCES (continued)

[11]

Low-dose CT (lung screen) — 94% / 73%. National Lung Screening Trial Research Team. Results of Initial Low-Dose Computed Tomographic Screening for Lung Cancer. N Engl J Med. 2013;368:1980–1991. doi:10.1056/NEJMoa1209120 — sensitivity 93.8%, specificity 73.4% (high false-positive rate).

[12]

Procalcitonin (bacterial sepsis) — 77% / 79%. Wacker C, Prkno A, Brunkhorst FM, Schlattmann P. Procalcitonin as a diagnostic marker for sepsis: a systematic review and meta-analysis. Lancet Infect Dis. 2013;13(5):426–435.

[13]

NT-proBNP (heart failure) — ~96% / ~47%. Diagnostic Utility of NT-proBNP and CRP in Diagnosing Heart Failure in Patients with Acute Hypoxemic Respiratory Failure. PMC7051103 — sensitivity 95.6%, specificity 46.8%; high negative predictive value (a rule-out marker).

[14]

COVID-19 rapid antigen (vs RT-PCR) — 70% / 98%. Performance of Rapid Antigen Tests for COVID-19 Diagnosis: A Systematic Review and Meta-Analysis. PMC8774565, 2022 — pooled sensitivity 70%, specificity 98%; ≈82% sensitivity in symptomatic patients.

[15]

TSH (thyroid dysfunction) — ~98% / ~92%. U.S. Preventive Services Task Force. Screening for Thyroid Dysfunction: Recommendation Statement. Ann Intern Med. 2015 (M15-0483) — serum TSH sensitivity ≈98%, specificity ≈92% to confirm clinically suspected thyroid disease; first-line test, abnormal result confirmed with free T4.

[16]

PSA (prostate cancer) — ~86% / ~33%. Meta-analyses: hospital setting, PSA <4 ng/mL, sensitivity 0.92 / specificity 0.16 (Investig Clin Urol 2022); sub-Saharan review, 4–10 ng/mL, 93.1% / 29.3% (Afr J Urol 2023). Sensitive but poorly specific; threshold-dependent and contested.

[17]

CRP (bacterial infection) — ~80% / ~67%. Lubell Y, et al. Performance of CRP and procalcitonin to distinguish viral from bacterial and malarial causes of fever in Southeast Asia. BMC Infect Dis. 2015 — at 20 mg/L, 86% / 67%; bacterial pneumonia (PERCH) 77% / 82%. Rises with cut-off.

[18]

HbA1c & fasting plasma glucose (diabetes) — 51% / 96% and 49% / 98%. Comparison of diagnostic accuracy for diabetes diagnosis: a systematic review and network meta-analysis. Front Med. 2023 — vs OGTT reference; both highly specific but insensitive.

REFERENCES (continued)

Related works

[S1]

Yoshimoto Cube — two stellated rhombic dodecahedra fold into a cube, each half its volume; in the Museum of Modern Art’s permanent collection since 1982. en.wikipedia.org/wiki/Yoshimoto_Cube ; store.moma.org

[S2]

Villeponteau B. Unified Quantum Substructures for Spacetime, Quarks, Leptons, and Bosons (the Triad Model). SSRN preprint 4492057.

[S3]

Vangelatos Z, Melissinaki V, Farsari M, Komvopoulos K, Grigoropoulos C. Intertwined microlattices greatly enhance the performance of mechanical metamaterials. Mathematics and Mechanics of Solids 2019;24(8):2636–2648. doi 10.1177/1081286519848041

[S4]

Pan K, Bricker WP, Ratanalert S, Bathe M. Structure and conformational dynamics of scaffolded DNA origami nanoparticles. Nucleic Acids Research 2017;45(11):6284–6298. doi 10.1093/nar/gkx378

[S5]

Grego and Gergő Kiss. Számozási kísérlet a stellált rombikus dodekaéderen (A numbering experiment on the stellated rhombic dodecahedron); GeoGebra construction by Lajos Szilassi.

[S6]

Földvári GG (Grego). Coefficial Divisibility — Multimorphism, Transdimension and Singularity. grego.hu/CoefficialDivisibility.pdf

[S7]

On-Line Encyclopedia of Integer Sequences: A387889, A387890 (first differences of consecutive odd / even perfect powers); A389262 (least k such that more than half the permutations of n elements have longest cycle ≤ k). tinyurl.com/gregomat ; GooglyCube, googlycube.com

[S8]

Magic star — the hexagram is the smallest (lowest-order) magic star. Wikipedia, ‘Magic star’.

REFERENCES (continued)

Clinical sources

[C1]

National Organization for Rare Disorders (NORD). Addison’s Disease. NORD Rare Disease Database, rarediseases.org. (Report acknowledgment: Maria I. New, MD.)

[C2]

Ten S, New M, Maclaren N. Clinical review 130: Addison’s disease. J Clin Endocrinol Metab 2001;86:2909–2922.

[C3]

Erickson QL, Faleski EJ, Koops MK, et al. Addison’s disease: the potentially life-threatening tan. Cutis 2000;66:72–74.

[C4] Paterson JR, et al. Delayed diagnosis of Addison’s disease. Ann Clin Biochem 1990;27:378–381.

[C5]

Anglin RE, Rosebush PI, Mazurek MF. The neuropsychiatric profile of Addison’s disease: revisiting a forgotten phenomenon. J Neuropsychiatry Clin Neurosci 2006;18:450–459.

Hans Holbein the Younger, “The Ambassadors” (1533), The National Gallery, London

COLOPHON

STAR FACE is my transdimensional-polyhedron model: symmetry stands for the governing laws of science; the projection of three dimensions onto two stands for cognitive development; and the combinatorics stands for the interaction of caregiver, patient, and diagnostic tools. The equilibrial sieve is the model's first filter, keeping only what is internally consistent. The second sieve is unambiguity, the third is reliability. The three are governed by the principle of SUMMETRY. This volume documents the families and groupings and the threestage sieve (equilibrium, unambiguity and reliability), closing with the masking landscape of the twelve pyramids and an open proposal: that this structure may offer a vocabulary for the diagnosis of rare disease. That correspondence is put forward for future research, not as a settled clinical result.

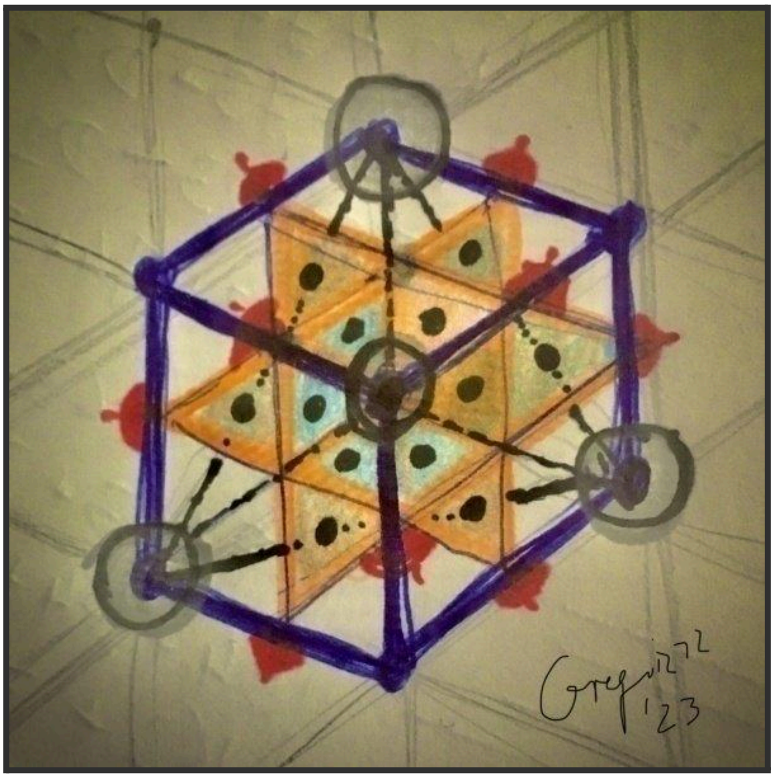

The author's original sketch: DIAMOND — Grego, 2023

DOI: https://doi.org/10.5281/zenodo.22259868

June 2026

Manuscript: 2016–2026

Web URL: https://www.grego.hu/star

Contact: gfoldvari@alumni.berklee.edu, gfoldvari@gmail.com

Entire site designed and all original music composed and played by Grego

Musicians: Vilmos Jávori (d), Béla Lattmann (bg), Attila László (eg), Kornél Horváth (pe), Tibor Szűcs (ag), Bea Tisza (v), János Ávéd (as), Ernő Hock (ab), Bence Baranyi (d), Grego (pi) Cantus Corvinus (ch), László Mező (ce), excerpts played by Grego (pi): Bach, Schubert, Moussorgsky